© 2016. Published by The Company of Biologists Ltd | Development (2016) 143, 1547-1559 doi:10.1242/dev.129676

RESEARCH ARTICLE

Restricting calcium currents is required for correct fiber type specification in skeletal muscle

Nasreen Sultana[1], Beatrix Dienes[2], Ariane Benedetti[1], Petronel Tuluc[3], Peter Szentesi[2], Monika Sztretye[2], Johannes Rainer[4], Michael W. Hess[5], Christoph Schwarzer[6], Gerald J. Obermair[1], Laszlo Csernoch[2] and Bernhard E. Flucher[1,*]

ABSTRACT

Skeletal muscle excitation-contraction (EC) coupling is independent of calcium influx. In fact, alternative splicing of the voltage-gated calcium channel $Ca_V1.1$ actively suppresses calcium currents in mature muscle. Whether this is necessary for normal development and function of muscle is not known. However, splicing defects that cause aberrant expression of the calcium-conducting developmental $Ca_V1.1e$ splice variant correlate with muscle weakness in myotonic dystrophy. Here, we deleted *$Ca_V1.1$* (*Cacna1s*) exon 29 in mice. These mice displayed normal overall motor performance, although grip force and voluntary running were reduced. Continued expression of the developmental $Ca_V1.1e$ splice variant in adult mice caused increased calcium influx during EC coupling, altered calcium homeostasis, and spontaneous calcium sparklets in isolated muscle fibers. Contractile force was reduced and endurance enhanced. Key regulators of fiber type specification were dysregulated and the fiber type composition was shifted toward slower fibers. However, oxidative enzyme activity and mitochondrial content declined. These findings indicate that limiting calcium influx during skeletal muscle EC coupling is important for the secondary function of the calcium signal in the activity-dependent regulation of fiber type composition and to prevent muscle disease.

KEY WORDS: Voltage-gated calcium channel, Skeletal muscle excitation-contraction coupling, Muscle fiber type specification, Mouse

INTRODUCTION

Calcium is the principal second messenger regulating skeletal muscle contraction, growth and differentiation. In excitation-contraction (EC) coupling, cytoplasmic calcium levels are rapidly increased in response to action potentials and the magnitude of these calcium signals regulates the force of contraction. In skeletal muscle, voltage-gated calcium channels ($Ca_V1.1$) and calcium release channels (type 1 ryanodine receptors, RyR1) are physically coupled to one another so that voltage-dependent activation of $Ca_V1.1$ can directly activate opening of the RyR1. In mature muscles, calcium is released from the sarcoplasmic reticulum (SR) calcium stores, whereas calcium influx is dispensable for skeletal muscle EC coupling (Melzer et al., 1995). Actually, calcium currents through the major $Ca_V1.1a$ splice variant are small and activate slowly, only at strong membrane depolarizations.

Interestingly, during maturation of mammalian skeletal muscles activity-dependent calcium influx is actively suppressed by alternative splicing of $Ca_V1.1$. In fetal muscles, exclusion of exon 29 produces a $Ca_V1.1e$ channel variant that conducts sizable L-type calcium currents and activates in parallel to SR calcium release at physiological voltages (Tuluc et al., 2009). However, after birth, the developmental $Ca_V1.1e$ splice variant is almost completely replaced by the adult, poorly conducting $Ca_V1.1a$ splice variant that includes exon 29 (Flucher and Tuluc, 2011; Tang et al., 2012). Why calcium influx is present in developing muscle but is then curtailed in mature skeletal muscles is not known. Conversely, it remains to be determined whether continued expression of the calcium-conducting $Ca_V1.1e$ splice variant alters contractile properties of mature skeletal muscles.

In addition to their primary role in EC coupling, activity-induced calcium signals in skeletal muscle are important for maintaining calcium homeostasis and for the regulation of muscle growth and differentiation. For example, calcium signals regulate the transcription of genes involved in the adaptive response to exercise (Bassel-Duby and Olson, 2006). Therefore, the tight control of calcium influx by alternative splicing of the $Ca_V1.1$ channel is probably important for tuning muscle function to varying activity levels. Conversely, calcium influx through $Ca_V1.1e$ channels in mature muscles might be harmful. Abnormal expression of the embryonic, calcium-conducting $Ca_V1.1e$ splice variant in myotonic dystrophy type 1 (DM1) patients correlates with their degree of muscle weakness (Tang et al., 2012). Moreover, aberrant splicing of calcium channels and transporters in cultured myotubes from DM1 patients leads to altered intracellular calcium signaling (Santoro et al., 2014), and experimentally induced skipping of exon 29 aggravated the disease phenotype in muscles of a myotonia mouse model (Tang et al., 2012).

To identify the physiological importance of curtailing calcium influx through $Ca_V1.1$ channels in adult skeletal muscle and to reveal a possible involvement of aberrant calcium signaling in DM1, we generated a genetic mouse model in which exon 29 has been permanently deleted. As expected, skeletal muscles of $Ca_V1.1^{\Delta E29/\Delta E29}$ knockout mice experienced increased calcium influx during EC coupling and at rest. In addition, their contractile properties were altered, calcium-activated downstream regulators were upregulated, and the fiber type composition was shifted towards slower fiber types. However, mitochondrial content and oxidative enzyme activity were reduced. Together, these findings

[1]Department of Physiology and Medical Physics, Medical University Innsbruck, Innsbruck 6020, Austria. [2]Department of Physiology, Faculty of Medicine, University of Debrecen, Debrecen 4032, Hungary. [3]Department of Pharmacology, University of Innsbruck, Innsbruck 6020, Austria. [4]Division of Molecular Pathophysiology, Biocenter, Medical University Innsbruck, Innsbruck 6020, Austria. [5]Division of Histology and Embryology, Medical University Innsbruck, Innsbruck 6020, Austria. [6]Department of Pharmacology, Medical University Innsbruck, Innsbruck 6020, Austria.

*Author for correspondence (Bernhard.E.Flucher@i-med.ac.at)

Received 11 August 2015; Accepted 29 February 2016

Development (2016) 143, 1547-1559 doi:10.1242/dev.129676

indicate that chronically increased calcium influx through the developmental $Ca_V1.1e$ isoform has little effect on EC coupling, but disturbs the normal regulation of muscle fiber type composition. Furthermore, the increased calcium influx causes mitochondrial damage and may thus contribute to muscle wasting in DM1. Conversely, these results suggest that, during normal development, limiting L-type calcium currents is important to enable the proper specification of fiber type composition and to protect the muscles from calcium-induced damage.

RESULTS

Selective deletion of *$Ca_V1.1$* exon 29 prevents the developmental switch from the $Ca_V1.1e$ to the $Ca_V1.1a$ isoform

In order to study the importance of the isoform switch from the calcium-conducting developmental $Ca_V1.1e$ splice variant to the poorly conducting adult $Ca_V1.1a$ splice variant we generated a mouse model with a constitutive knockout of exon 29 of the *$Ca_V1.1$* (*Cacna1s*) gene (Fig. 1A). We reasoned that because the short transcript *$Ca_V1.1e$* is predominant during fetal development, *$Ca_V1.1^{\Delta E29}$* mice would develop normally up to birth, but that the aberrant continuing expression of the high-conductance developmental calcium channel splice variant throughout postnatal development and adult life would reveal any influence of the extra calcium influx on EC coupling and/or other calcium-mediated signaling processes regulating muscle growth and differentiation. Furthermore, the *$Ca_V1.1^{\Delta E29}$* mouse will expose whether aberrant splicing of $Ca_V1.1$ is itself sufficient to cause a disease phenotype reminiscent of DM1.

Heterozygous *$Ca_V1.1^{+/\Delta E29}$* and homozygous *$Ca_V1.1^{\Delta E29/\Delta E29}$* mice were viable, they developed normally, and home cage activity of *$Ca_V1.1^{\Delta E29}$* mice was not significantly different from that of wild-type siblings (Fig. 1B, Fig. S1A). Expression of the two *$Ca_V1.1$* transcripts at different developmental stages was analyzed in the predominantly slow/oxidative soleus muscle, the predominantly fast/glycolytic extensor digitorum longus (EDL) muscle, and the mixed diaphragm muscle. Quantitative RT-PCR demonstrated that wild-type fetal muscles express moderate levels of both splice variants, with a higher proportion of the splice variant lacking exon 29 ($Ca_V1.1e$) (Fig. 1C). After birth, wild-type muscles experienced a strong upregulation of the *$Ca_V1.1a$* transcript, whereas expression of the *$Ca_V1.1e$* transcript declined to less than 3% in 16-week-old mice. In muscles of ageing mice (15-18 months), total *$Ca_V1.1$* transcript levels declined but the overall predominance of the $Ca_V1.1a$ variant was maintained. As expected, in homozygous *$Ca_V1.1^{\Delta E29/\Delta E29}$* mice the *$Ca_V1.1e$* transcript was found exclusively. At all developmental stages its expression levels resembled those of total *$Ca_V1.1$* transcripts in wild-type mice. Western blot analysis confirmed normal expression levels of total $Ca_V1.1$ protein in soleus (Fig. 1D). However, in EDL muscle total $Ca_V1.1$ protein was reduced. This might, at least in part, reflect a reduced content of triad junctions due to the fiber type shift observed in *$Ca_V1.1^{\Delta E29}$* muscles (see below).

Aberrant expression of the developmental $Ca_V1.1e$ isoform in mature muscles is not sufficient to cause severe myotonic dystrophy symptoms in mice

Because aberrant expression of $Ca_V1.1e$ in adults has been linked to the DM1 phenotype in mouse and human (Santoro et al., 2014; Tang et al., 2012), we subjected *$Ca_V1.1^{\Delta E29}$* mice at 2 and 8 months of age to a range of behavioral tests to examine different aspects of muscle performance (Fig. 2). A wire hang test was used to assess muscle strength. Endurance was tested by making the mice run on a treadmill at accelerating speed until exhaustion. Overall motor performance was examined with the Rotarod test. In none of these tests was a significant difference in the performance of wild-type, heterozygous *$Ca_V1.1^{+/\Delta E29}$* and homozygous *$Ca_V1.1^{\Delta E29/\Delta E29}$* mice observed. However, directly measuring grip strength revealed that the grip force of the front paws was significantly reduced in homozygous *$Ca_V1.1^{\Delta E29/\Delta E29}$* mice (Fig. 2D). Finally, voluntary running of the mice in a running wheel was recorded over the period of 7 days. Both the distance run and the duration the mice spent running per day were significantly reduced in homozygous *$Ca_V1.1^{\Delta E29/\Delta E29}$* mice compared with wild-type controls (Fig. 2E). These behavioral and functional analyses indicate that aberrant expression of $Ca_V1.1e$ alters muscle performance without causing severe motor deficits as assessed in tests that revealed the disease phenotype in other DM mouse models (Gomes-Pereira et al., 2011). Also, histological staining of muscle sections did not reveal an increase in centrally located nuclei in *$Ca_V1.1^{\Delta E29/\Delta E29}$* muscles (Fig. S1B).

Aberrant expression of the developmental $Ca_V1.1e$ isoform in mature muscles alters the contractile properties of isolated slow and fast muscles

Because the reduced grip force and voluntary running indicated altered muscle performance, we next determined the contractile properties directly in isolated mouse muscles. The contractile force of soleus and EDL muscles was recorded in response to a single electrical stimulus (twitch) and in response to high-frequency trains of stimuli (tetanus) (Fig. 3A). Both were significantly reduced in both muscles types of *$Ca_V1.1^{\Delta E29/\Delta E29}$* mice (Fig. 3B, Table 1). The relative decline of muscle force during a continuous series of repetitive tetanic stimulations is a measure of the fatigability of the muscle (Fig. 3C). Slow soleus muscles are more fatigue resistant than fast EDL muscles. In *$Ca_V1.1^{\Delta E29/\Delta E29}$* mice, both muscle types display significantly reduced fatigue compared with wild-type controls (Fig. 3D, Table 1). Finally the tetanic fusion frequency was assessed by recording tetanic force during a series of stimulus trains of increasing frequency (Fig. 3E). *$Ca_V1.1^{\Delta E29/\Delta E29}$* muscles reached the half-maximal value and the plateau of contractile force at lower frequencies than control muscles. This is reflected by a left shift of the force frequency curve (Fig. 3F) and a reduction of the frequency of the half-maximal tetanic force (Fig. 3G) in both soleus and EDL muscles. Together, these tests on isolated muscles demonstrate that expression of $Ca_V1.1e$ in adult *$Ca_V1.1^{\Delta E29/\Delta E29}$* mice significantly reduces the contractile force, increases the fatigue resistance, and lowers the tetanic fusion frequency of slow and fast muscles.

Aberrant expression of the developmental $Ca_V1.1e$ isoform in mature muscles alters calcium signals during EC coupling and in resting muscle fibers

To clarify the cellular mechanisms underlying the altered muscle properties of *$Ca_V1.1^{\Delta E29/\Delta E29}$* mice we analyzed calcium currents and cytoplasmic calcium signals directly in isolated flexor digitorum brevis (FDB) muscle fibers using several experimental paradigms. First, combined patch-clamp and cytoplasmic calcium recording was performed in FDB fibers loaded with the fluorescent calcium indicator Rhod-2. In line with the current properties of the $Ca_V1.1e$ splice variant previously determined in reconstituted dysgenic myotubes (Tuluc et al., 2009), *$Ca_V1.1^{\Delta E29/\Delta E29}$* FDB fibers displayed sizable calcium currents starting at test potentials of −30 mV (Fig. 4A). Under the same conditions (1.8 mM extracellular calcium, 100 ms test pulses), control FDB fibers did

Development (2016) 143, 1547-1559 doi:10.1242/dev.129676

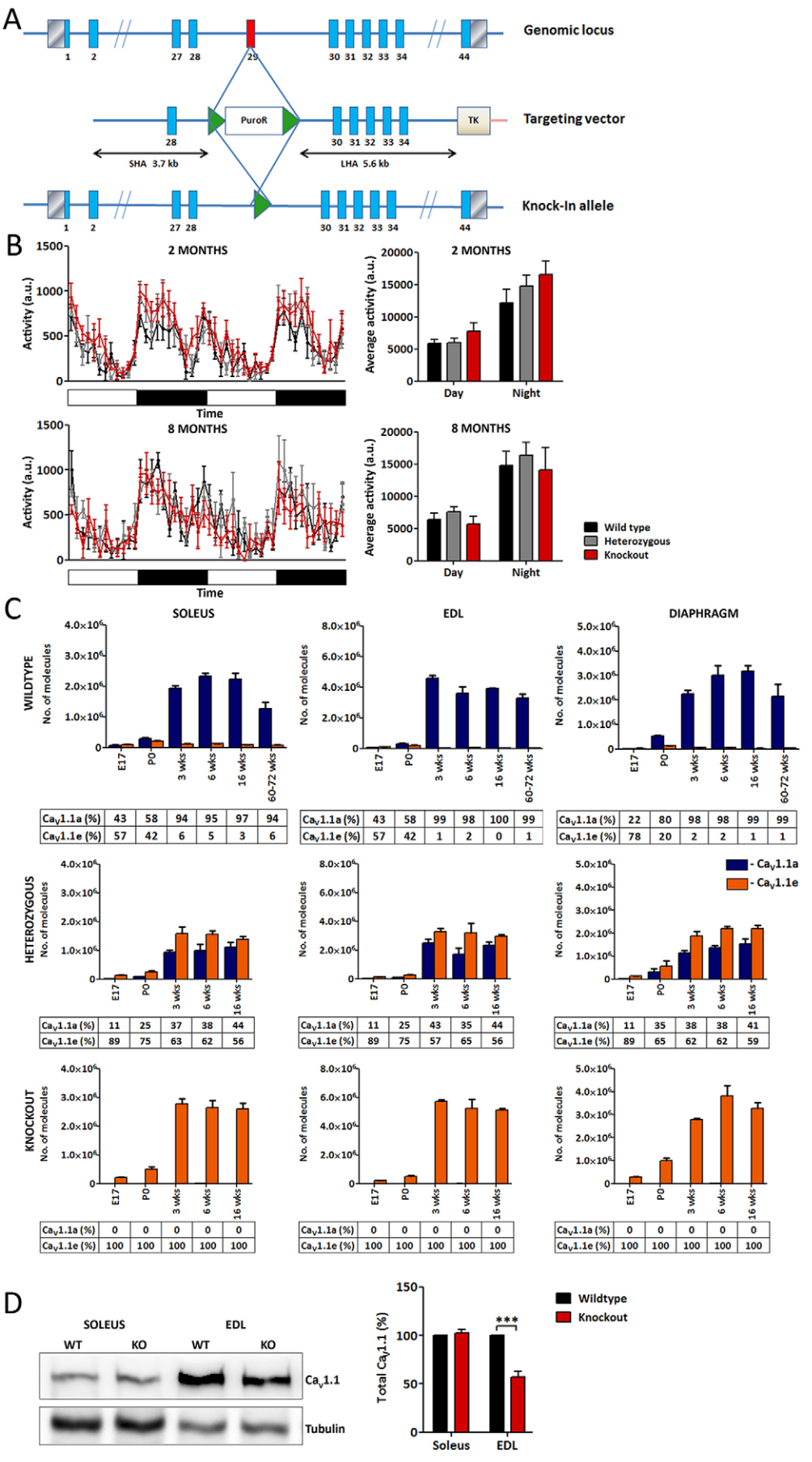

Fig. 1. Characterization of the $Ca_V1.1^{\Delta E29}$ mouse. (A) Targeting strategy for generating the $Ca_V1.1$ exon 29 knockout allele. (B) Voluntary home cage activity at 2 and 8 months of age is similar in $Ca_V1.1^{\Delta E29/\Delta E29}$ mice compared with wild-type and $Ca_V1.1^{+/\Delta E29}$ siblings (*N*=5). (C) Expression levels of $Ca_V1.1a$ and $Ca_V1.1e$ mRNAs in wild-type, $Ca_V1.1^{+/\Delta E29}$ and $Ca_V1.1^{\Delta E29/\Delta E29}$ mice were measured by quantitative RT-PCR (TaqMan) in soleus, EDL and diaphragm muscle at different developmental stages (*N*=3). Numbers beneath show the fractional content of the two $Ca_V1.1$ transcripts. (D) Western blot analysis of total $Ca_V1.1$ protein (both splice variants) in soleus and EDL muscle of wild-type and $Ca_V1.1^{\Delta E29}$ mice (*N*=3; ***P<0.001). Mean±s.e.m. See also Fig. S1.

Development (2016) 143, 1547-1559 doi:10.1242/dev.129676

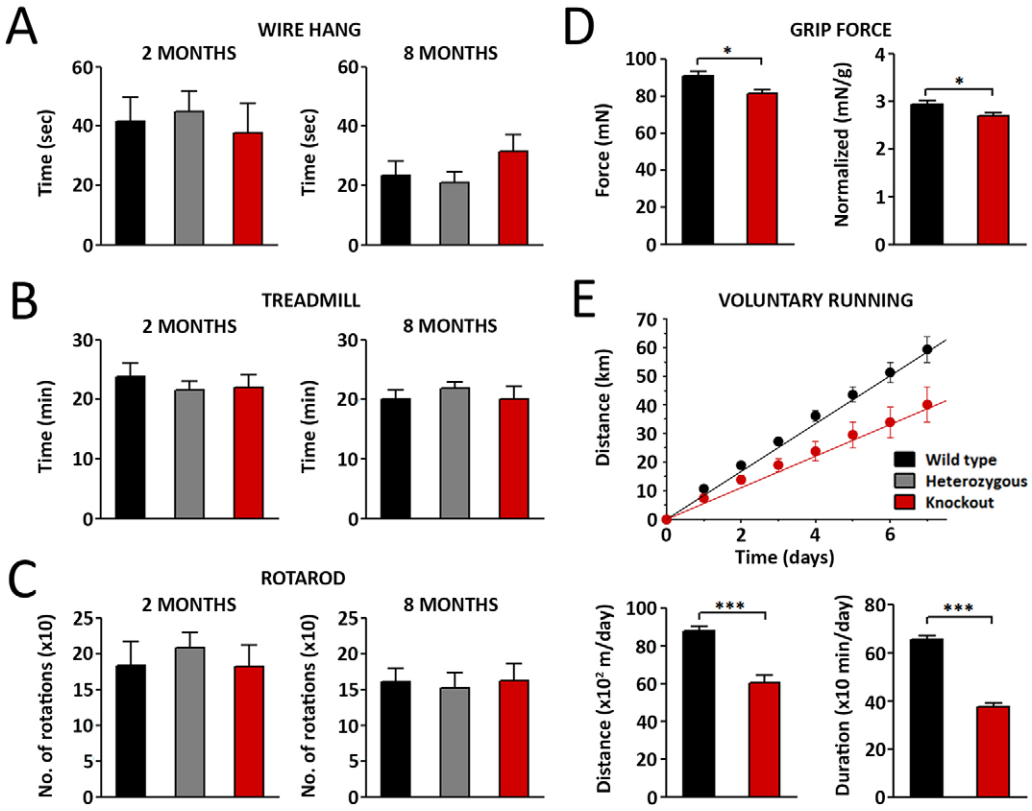

Fig. 2. $Ca_V1.1^{\Delta E29}$ mice show normal motor performance but reduced muscle strength. (A-C) Strength, endurance and motor skills were examined in wild-type, $Ca_V1.1^{+/\Delta E29}$ and $Ca_V1.1^{\Delta E29/\Delta E29}$ mice using the wire hang test (A), treadmill running to exhaustion (B) and the Rotarod test (C). At 2 and 8 months of age, the performance of $Ca_V1.1^{\Delta E29}$ mice did not differ from that of the other genotypes (N=5-8; P>0.05). (D) Direct measurement of front paw strength revealed reduced grip force (both in absolute value and force normalized to body weight) in 6-month-old $Ca_V1.1^{\Delta E29/\Delta E29}$ mice compared with wild-type siblings (N=5-8; *P<0.05). (E) Analysis of voluntary wheel running over a period of 7 days showed that the running distance and duration per day were decreased in $Ca_V1.1^{\Delta E29/\Delta E29}$ mice compared with the wild type (N=8; ***P<0.001). Mean±s.e.m.

not display measurable currents at any test potential. In order to compare voltage sensitivity between the two genotypes, recordings in control fibers were repeated using 5 mM extracellular calcium and 500 ms test pulses. The current-voltage and current-conductance curves indicate that in $Ca_V1.1^{\Delta E29/\Delta E29}$ fibers half-maximal current activation is shifted by 38.5±3.1 mV in the hyperpolarizing direction (Fig. 4B). Accordingly, the simultaneously recorded calcium transients in $Ca_V1.1^{\Delta E29/\Delta E29}$ fibers showed a pronounced voltage-dependent component that peaked at −20 mV and declined in parallel with the current density at positive potentials (Fig. 4C).

From the calcium transients the total calcium flux (influx and SR release) during the depolarizing pulses was calculated (Fig. 4A lower trace, Fig. S2). These calcium flux traces characteristically showed an early peak followed by a steady-state plateau phase (Szentesi et al., 1997). In control muscle, the voltage dependence of both the peak and plateau calcium fluxes displayed a monotonic increase, which could be fitted with a two-state Boltzmann function. This is consistent with a model of skeletal muscle EC coupling in which both parameters of the calcium flux (peak and plateau) represent a single process, i.e. calcium release from the SR. In $Ca_V1.1^{\Delta E29/\Delta E29}$ muscle fibers, the peak calcium flux behaved like that in controls, whereas the voltage dependence of the plateau flux was non-monotonous. At intermediate voltages the plateau flux was significantly larger than that of controls. Thus, the additional component in $Ca_V1.1^{\Delta E29/\Delta E29}$ muscles compared with controls corresponds to voltage-dependent calcium influx, which peaks at −20 mV where most $Ca_V1.1e$ channels are activated and then decreases in parallel with the declining driving force at positive membrane potentials. Together, these analyses clearly demonstrate that, during EC coupling, muscle fibers of $Ca_V1.1^{\Delta E29/\Delta E29}$ mice experience increased calcium signals due to a substantial component of calcium influx that is not observed in muscle fibers of wild-type mice.

In addition to its immediate role in EC coupling, this extra calcium influx in $Ca_V1.1^{\Delta E29/\Delta E29}$ mice might alter the calcium homeostasis in muscle cells. Analysis of cytoplasmic calcium concentrations in Fura-2-loaded isolated FDB fibers revealed no difference in resting calcium levels of $Ca_V1.1^{\Delta E29/\Delta E29}$ mice compared with wild-type controls (45.77±0.96 nM and 46.14±1.14 nM, respectively; P>0.5). Next, we examined a possible contribution of L-type calcium currents to refilling of SR calcium stores. Both SR depletion and refilling resulted in a robust cytoplasmic calcium transient (Fig. 4D), the relative magnitude of which was expressed as the external to SR calcium transient ratio. In wild-type muscle fibers this ratio was not affected by the application of the L-type calcium channel blocker nisoldipine. However, in $Ca_V1.1^{\Delta E29/\Delta E29}$ muscle fibers 5 µM nisoldipine dramatically reduced the ratio, indicating that in $Ca_V1.1e$-expressing muscle SR refilling is predominantly carried out by calcium influx through L-type channels (i.e. $Ca_V1.1e$).

Finally, the spontaneous occurrence of focal calcium transients – so called calcium sparklets – in resting muscle fibers was investigated. Because similar local calcium release events are exclusive to muscle cells expressing calcium-conducting Ca_V

Development (2016) 143, 1547-1559 doi:10.1242/dev.129676

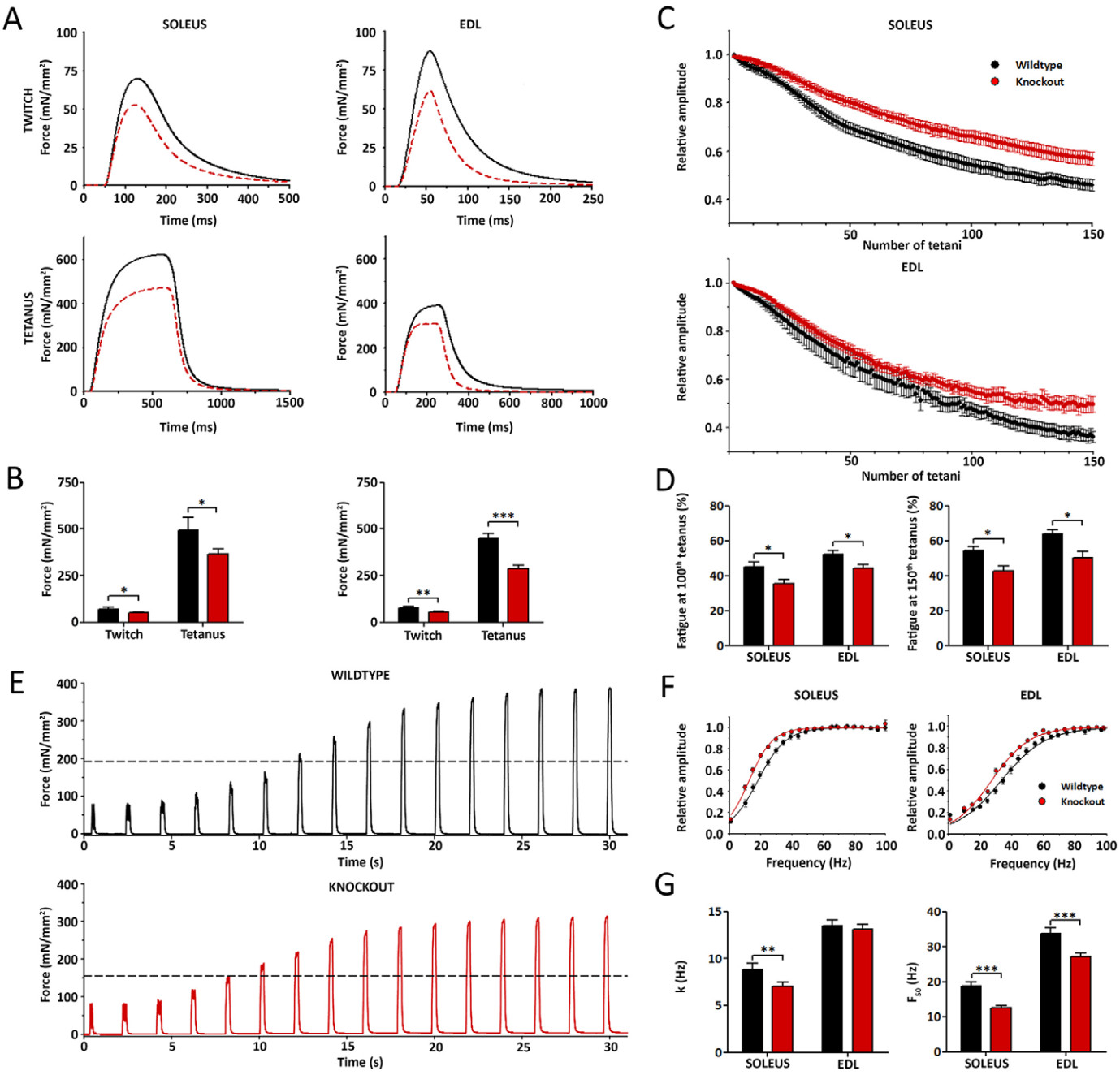

Fig. 3. Contractile properties of isolated slow and fast skeletal muscles are altered in $Ca_V1.1^{\Delta E29/\Delta E29}$ mice. (A) Representative recordings of twitch and tetanic contractions in isolated soleus and EDL muscles of 3- to 6-month-old wild-type (black; *N*=5) and $Ca_V1.1^{\Delta E29/\Delta E29}$ (red; *N*=15) mice. Muscle twitches were elicited by a single 2 ms supramaximal electrical pulse (top), tetani by stimulation trains at 100 Hz for 500 ms in soleus (lower left) or at 200 Hz for 200 ms in EDL (lower right). (B) Maximal twitch and tetanic forces are significantly reduced in $Ca_V1.1^{\Delta E29/\Delta E29}$ compared with control muscles (control *N*=5, $Ca_V1.1^{\Delta E29/\Delta E29}$ *N*=15). (C) Decline of maximal force during 150 repetitive tetani in soleus (upper) and EDL (lower) muscles of wild-type (black) and $Ca_V1.1^{\Delta E29/\Delta E29}$ (red) mice (stimulation as in A, repeated at 0.5 Hz; normalized to the first tetanus; control *N*=5, $Ca_V1.1^{\Delta E29/\Delta E29}$ *N*=15). (D) Relative reduction of force at the 100th and 150th tetanus was significantly lower in $Ca_V1.1^{\Delta E29/\Delta E29}$ than in wild-type muscles. (E) Representative force transients of isolated EDL muscle stimulated with increasing frequencies (10 to 85 Hz, with 0.5 Hz increment) from wild-type (black) and $Ca_V1.1^{\Delta E29/\Delta E29}$ (red) mice. Note that 50% of maximal force (dashed line) is reached at 40 Hz (seventh transient) in wild-type and at 30 Hz (fifth transient) in $Ca_V1.1^{\Delta E29/\Delta E29}$ muscles. (F) Relative force-frequency curves are left shifted in soleus (left) and EDL (right) muscles of $Ca_V1.1^{\Delta E29/\Delta E29}$ (red) compared with wild-type (black) mice. (G) The frequency required for producing half-maximal force was significantly lower in soleus and EDL muscles of $Ca_V1.1^{\Delta E29/\Delta E29}$ compared with wild type (control *N*=7, $Ca_V1.1^{\Delta E29/\Delta E29}$ *N*=12). **P*<0.05, ***P*<0.01, ****P*<0.001. Mean±s.e.m.

channels (e.g. $Ca_V1.2$ in cardiac myocytes), we hypothesized that aberrant expression of $Ca_V1.1e$ might also bring about calcium sparklets in mature muscle fibers of $Ca_V1.1^{\Delta E29/\Delta E29}$ mice. Indeed, isolated FDB fibers from $Ca_V1.1^{\Delta E29/\Delta E29}$ mice loaded with Fluo-8 AM displayed spontaneous calcium sparklet-like behavior (Fig. 4E). The average amplitude of these calcium sparklets was 0.140±0.001 [ΔF/F]. The average amplitude, full width and half maxima of these calcium sparklets resembled those described by Rodríguez et al. (2014). In 5 mM extracellular calcium, these calcium sparklets occurred at a frequency of 0.724 ±0.211 10^{-3} s^{-1} mm^{-1}. When the extracellular calcium concentration was reduced to 1.8 mM, or when L-type calcium

Development (2016) 143, 1547-1559 doi:10.1242/dev.129676

Table 1. Contractile properties of soleus and EDL muscles of $Ca_V1.1^{\Delta E29/\Delta E29}$ and wild-type mice

	Soleus			EDL		
Property	Wild type (*N*=5)	Knockout (*N*=15)		Wild type (*N*=5)	Knockout (*N*=15)	
Twitch force (mN/mm^2)	70.3±10.0	50.2±4.8	*P*<0.05	78.0±7.3	54.2±4.1	*P*<0.01
Tetanic force (mN/mm^2)	492.4±67.4	368.1±22.8	*P*<0.05	447.6±27.3	289.1±19.3	*P*<0.001
Fatigue (100th tetanus) %	45.2±2.8	35.3±2.7	*P*<0.05	52.1±2.3	44.9±2.2	*P*<0.05
Fatigue (150th tetanus) %	54.2±2.4	42.8±2.8	*P*<0.05	64.0±2.3	50.4±3.3	*P*<0.05
Force-frequency (slope, k)	9.20±0.67	6.90±0.45	*P*<0.01	13.74±0.67	12.90±0.54	*P*>0.05
Force-frequency (F_{50}, Hz)*	19.74±0.85	11.97±0.44	*P*<0.001	34.75±1.61	27.09±1.02	*P*>0.001

Values represent mean±s.e.m.
*Frequency of half-maximal force.

channels were blocked with 10 µM nisoldipine, the calcium sparklets were completely abolished, indicating their dependence on calcium influx through $Ca_V1.1e$. In wild-type control muscle fibers no such calcium release events were observed in normal or high extracellular calcium concentrations. Together, these findings demonstrate that calcium influx through the $Ca_V1.1e$ splice variant not only alters calcium handling during EC coupling and during refilling of SR calcium stores, but also causes spontaneous calcium signals in resting intact muscle fibers.

Muscles of $Ca_V1.1e$-expressing mice display an altered fiber type composition and oxidative metabolism

In skeletal muscle, calcium signals also regulate activity-dependent control of muscle growth and fiber type specification. Moreover, the observed changes in contractile properties – decreased force, increased fatigue resistance and lower tetanic fusion frequency – are all reminiscent of the differences between fast and slow muscle types. Therefore, we hypothesized that the altered calcium signaling in $Ca_V1.1^{\Delta E29/\Delta E29}$ mice might affect contractile properties indirectly by a dysregulation of fiber type specification.

To analyze the fiber type composition of slow and fast muscles in wild-type and $Ca_V1.1^{\Delta E29/\Delta E29}$ mice, we immunostained sections of soleus and EDL muscle with antibodies against specific myosin heavy chain isoforms. The representative images in Fig. 5A,D demonstrate a substantial shift towards slower fiber types in both soleus and EDL muscles of $Ca_V1.1^{\Delta E29/\Delta E29}$ mice. Soleus muscles of $Ca_V1.1^{\Delta E29/\Delta E29}$ mice experienced a 48% increase in the fraction of type I fibers, mainly at the cost of type IIA and mixed fibers (Fig. 5A-C). In EDL muscle of $Ca_V1.1^{\Delta E29/\Delta E29}$ mice the fraction of type IIB fibers was reduced by 26%, whereas the fractions of IIA, IIX and mixed fibers increased 2- to 3-fold (Fig. 5D-F). Type I fibers were not detected in $Ca_V1.1^{\Delta E29/\Delta E29}$ EDL muscles. These findings indicate that expression of the calcium-conducting $Ca_V1.1e$ splice variant in skeletal muscles of adult $Ca_V1.1^{\Delta E29/\Delta E29}$ mice causes a substantial shift in fiber type composition towards slower fiber types.

Aberrant expression of $Ca_V1.1e$ in mature skeletal muscle causes mitochondrial damage

A slower fiber type composition is expected to be accompanied by an increase in oxidative metabolism. Indeed, staining of succinate dehydrogenase (SDH) in soleus and EDL muscles of 7-week-old $Ca_V1.1^{\Delta E29/\Delta E29}$ mice revealed a marked increase in SDH activity compared with wild-type controls (Fig. 6A). In soleus, a loss of fibers with lower SDH activity was evident, probably reflecting the increase in type I fibers relative to type IIA fibers. In EDL, an increase in high SDH activity fibers occurred, consistent with the increased fraction of oxidative IIA fibers relative to glycolytic fiber types (see Fig. 5). Unexpectedly, in 6- and 12-month-old $Ca_V1.1^{\Delta E29/\Delta E29}$ mice the SDH activity was significantly reduced compared with the wild type (Fig. 6B, Fig. S3A). The left shift of the intensity distribution diagrams was more pronounced in soleus, but it was still significant in EDL. It equally affected fibers with low and high SDH activity. Together, these results show that the initial increase of oxidative metabolism in young $Ca_V1.1^{\Delta E29/\Delta E29}$ mice is lost and even reversed at 6 months and older.

Because decreased SDH activity could arise from either a reduction in mitochondrial activity or content, we analyzed mitochondria in electron microscopy preparations. Consistent with the overall healthy state and normal motor performance of the $Ca_V1.1^{\Delta E29/\Delta E29}$ mice, electron microscopy did not reveal any defects in the myofibrils and EC coupling membranes (Fig. 6C). However, the mitochondria were distorted in $Ca_V1.1^{\Delta E29/\Delta E29}$ muscles. Morphometric analysis revealed that the mitochondrial content was significantly reduced in $Ca_V1.1^{\Delta E29/\Delta E29}$ mice to approximately half that in wild-type controls (Fig. 6D, Fig. S3B). This loss of intact mitochondria was paralleled by an increase in the fraction of damaged mitochondria up to 4.5-fold compared with wild-type controls, as well as a decrease in the average size of the healthy mitochondria. These findings explain the significantly reduced SDH activity observed in $Ca_V1.1^{\Delta E29/\Delta E29}$ compared with wild-type muscles of the same age.

Aberrant expression of $Ca_V1.1e$ changes key activity- and calcium-dependent regulators of fiber type specification and mitochondrial biogenesis

If the altered calcium signals in $Ca_V1.1e$-expressing muscles impact the regulation of fiber type specification this might be reflected in the activity and/or expression levels of major calcium- and activity-regulated signaling proteins. In skeletal muscle, the calcium-dependent protein phosphatase calcineurin (protein phosphatase 2B) and the calmodulin-dependent protein kinase II (CaMKII) decode fiber type-specific activation patterns and function as master regulators of fast to slow fiber type changes (Chin et al., 1998; Wu et al., 2001; Chin, 2005). Using a colorimetric phosphatase assay we show that steady-state calcineurin activity is significantly increased in $Ca_V1.1^{\Delta E29/\Delta E29}$ soleus and EDL muscles (Fig. 7A). Western blot analysis using a phospho-specific antibody demonstrated that the activated forms of all three CaMKII isoforms were significantly increased in cytoplasmic fractions of soleus muscle (Fig. 7B), whereas in EDL muscles no changes in CaMKII activation were observed. A differential activation of CaMKII in slow versus fast muscles is consistent with its suggested role in differentially decoding slow and fast muscle calcium signals (Tavi and Westerblad, 2011).

Interestingly, expression of their respective downstream transcriptional regulators, NFATC1 and HDAC4, in the cytoplasm and nuclei of $Ca_V1.1^{\Delta E29/\Delta E29}$ muscles was not altered (Fig. 7C,D, Fig. S4A,B). However, expression of peroxisome

Development (2016) 143, 1547-1559 doi:10.1242/dev.129676

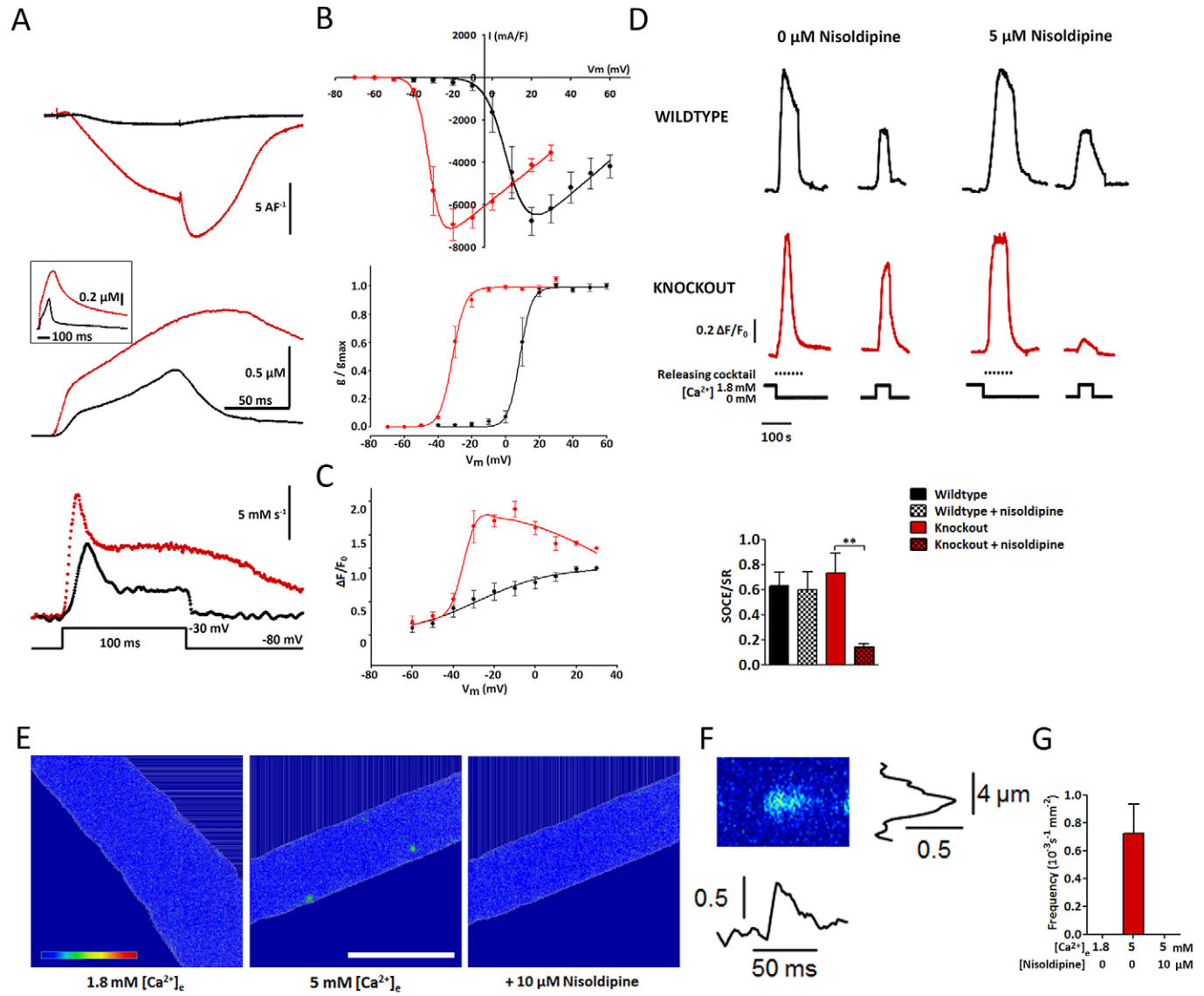

Fig. 4. Altered calcium signaling in isolated muscle fibers of $Ca_V1.1^{\Delta E29/\Delta E29}$ mice. Enzymatically isolated FDB fibers from 3- to 4-month-old $Ca_V1.1^{\Delta E29/\Delta E29}$ (red) and wild-type (black) mice were loaded with Rhod-2 (A-C) or Fluo-8 AM (D-G). (A) Representative voltage-clamp recording of calcium currents and parallel recording of cytoplasmic free calcium during a 100 ms depolarization to −30 mV. Bottom trace is the calculated total calcium flux. (B) Voltage dependence of peak current densities and conductance display the 38.5±3.1 mV shift of channel activation in $Ca_V1.1^{\Delta E29/\Delta E29}$ fibers. Note that $Ca_V1.1^{\Delta E29/\Delta E29}$ fibers were recorded in 1.8 mM extracellular calcium during 100 ms test pulses and control fibers in 5 mM calcium during 500 ms test pulses to experimentally normalize current densities. (C) Calcium transient amplitudes display a striking increase in $Ca_V1.1^{\Delta E29/\Delta E29}$ muscle fibers at intermediate voltages, indicative of the calcium influx through $Ca_V1.1e$. (D) Representative calcium recordings of wild-type and $Ca_V1.1^{\Delta E29/\Delta E29}$ fibers during an SR calcium release and reloading protocol. Note that the relative magnitude of the release and reloading transients is significantly decreased upon nisoldipine block of Ca_V1 channels in $Ca_V1.1^{\Delta E29/\Delta E29}$ but not in wild-type muscle (**P<0.01). (E) Representative confocal images of a resting $Ca_V1.1^{\Delta E29/\Delta E29}$ FDB fiber in 1.8 mM and 5 mM calcium. Spontaneous calcium release events occur only in 5 mM calcium and are blocked by addition of 10 µM nisoldipine. (F) Spatiotemporal properties in line-scan images identify the localized calcium signals as calcium sparklets. (G) The sparklets are sensitive to the extracellular calcium concentration and L-type channel block. n=32 images/N=4 animals (1.8 mM), n=183/N=7 (5 mM) and n=24/N=3 (5 mM+nisoldipine). Mean±s.e.m. See also Fig. S2.

proliferator-activated receptor γ co-activator 1α (*PGC1α*; *Ppargc1a*), a key downstream regulator of mitochondrial biogenesis and of oxidative metabolism in muscle (Handschin et al., 2007; Lin et al., 2002), was significantly increased in soleus muscle of $Ca_V1.1^{\Delta E29/\Delta E29}$ mice compared with wild-type controls (Fig. 7E). In EDL muscle, *PGC1α* expression was not significantly altered. Expression of *Six1*, a key regulator of the fast fiber program (Grifone et al., 2004; Wu et al., 2013), was not affected.

To further examine potential effects on the expression patterns of the slow and fast program and on mitochondrial biogenesis, Affymetrix expression profiling was performed on mRNA preparations from soleus and EDL muscles of wild-type and $Ca_V1.1^{\Delta E29/\Delta E29}$ mice. Although the analysis showed differential gene expression in soleus versus EDL muscles of both genotypes, comparison of wild-type versus $Ca_V1.1^{\Delta E29/\Delta E29}$ soleus and EDL muscles did not reveal any significant differences (Fig. S4C). Also, the specific analysis of genes involved in mitochondrial fusion and fission revealed only small differences between slow and fast muscles but not between wild-type and $Ca_V1.1^{\Delta E29/\Delta E29}$ mice. Thus, the increased calcium influx through $Ca_V1.1e$ chronically hyperactivates calcineurin, CaMKII and PGC1α signaling and, over time, produces the observed changes in fiber type composition

Development (2016) 143, 1547-1559 doi:10.1242/dev.129676

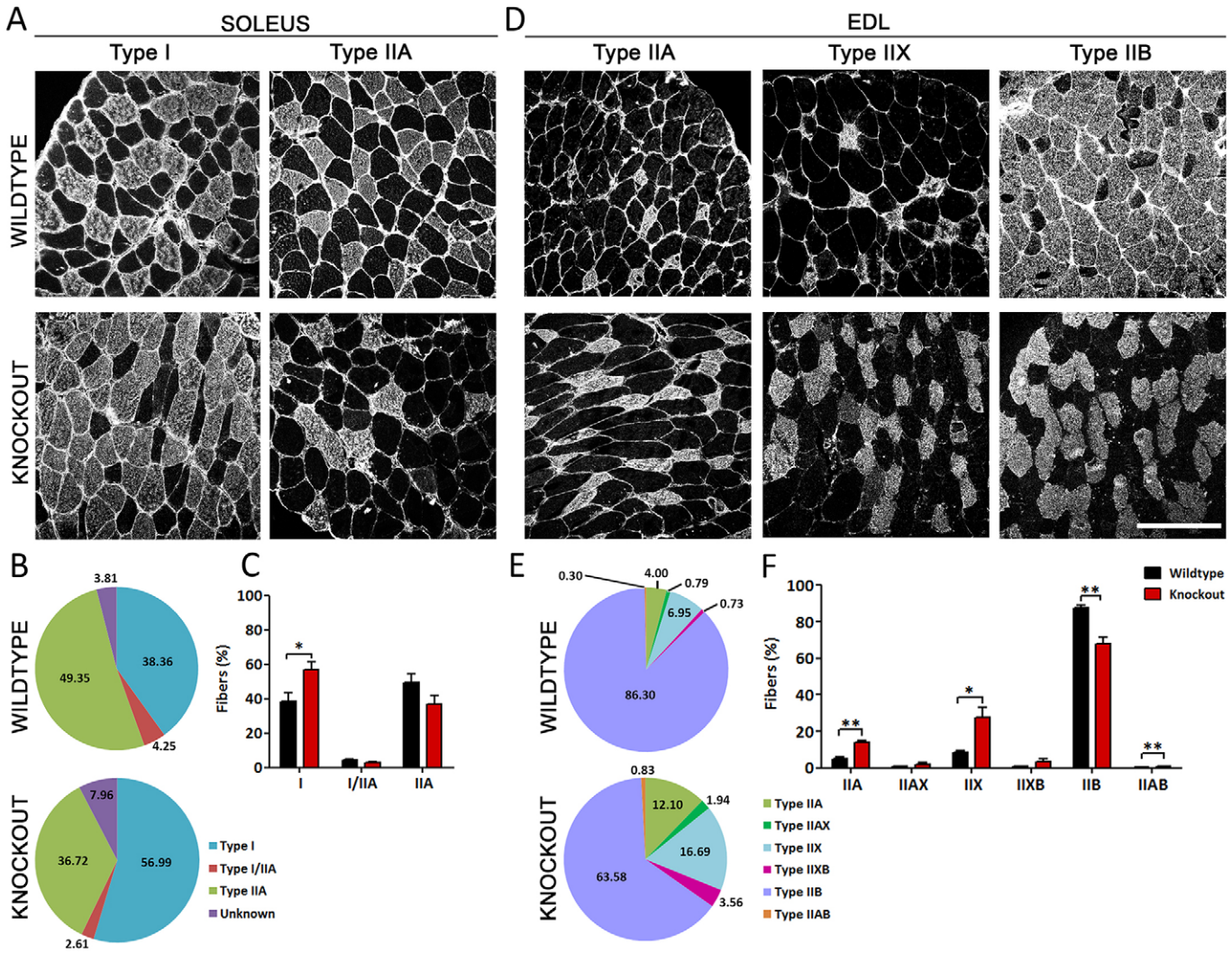

Fig. 5. Changes in fiber type composition and metabolic properties of soleus and EDL muscles in $Ca_V1.1^{\Delta E29/\Delta E29}$ mice. (A,D) Representative transverse sections of soleus and EDL muscles from 5- to 6-month-old wild-type and $Ca_V1.1^{\Delta E29/\Delta E29}$ mice immunostained with fiber type-specific myosin heavy chain antibodies. Scale bar: 100 µm. Note the increase of type I fibers and decrease of type IIA fibers in $Ca_V1.1^{\Delta E29/\Delta E29}$ soleus (A), and the increase of IIA and IIX fibers in parallel with the decrease of IIB fibers in $Ca_V1.1^{\Delta E29/\Delta E29}$ EDL (D). (B,E) The fractional redistribution of fiber types in $Ca_V1.1^{\Delta E29/\Delta E29}$ soleus and EDL muscles. (C,F) The relative magnitude and statistical significance of the changes in individual fiber types. N=3; *P<0.05, **P<0.01. Mean±s.e.m.

without, however, a major induction of the slow muscle gene program at basal activity levels in adult mice.

DISCUSSION

The developmental switch of $Ca_V1.1$ splice variants is important for the correct specification of skeletal muscle fiber types

Several lines of evidence at the molecular, functional and behavioral level demonstrate that the continued expression of the developmental $Ca_V1.1e$ splice variant in mature muscles of $Ca_V1.1^{\Delta E29/\Delta E29}$ mice alters the fiber type composition in the slow direction: (1) in soleus muscle the fraction of type I fibers increases at the expense of type IIA fibers, and in EDL muscles type IIA, IIX and mixed fibers increase at the expense of type IIB fibers; (2) in isolated soleus and EDL muscles maximal twitch and tetanic forces are reduced, fatigue resistance is increased, and tetanic fusion of contractions occurs at lower frequencies; (3) grip force and the duration of voluntary wheel running are reduced; (4) calcineurin and CaMKII activity and expression of PGC1α are upregulated. However, in mature mice the increased slow fiber content and the increased expression of PGC1α were no longer accompanied by the expected increase in oxidative enzyme activity, most likely because the increased calcium influx in $Ca_V1.1^{\Delta E29/\Delta E29}$ muscles also caused a severe loss of mitochondria.

The fiber type composition of skeletal muscles is primarily a genetically determined adaptation of muscle properties to their specific physiological functions. Furthermore, it is subject to continuous dynamic adaptation to altered demand. The changes in fiber type composition and contractile properties observed in the $Ca_V1.1^{\Delta E29/\Delta E29}$ mice are reminiscent of adaptations occurring in response to endurance training. The magnitude of the observed shift in fiber type composition is within the range observed in mice subjected to stringent endurance training protocols (Allen et al., 2001; Krüger et al., 2013). However, neither monitoring home cage activity nor the behavioral tests revealed increased spontaneous activity. If anything, $Ca_V1.1^{\Delta E29/\Delta E29}$ mice spent less time voluntarily running than wild-type controls. Therefore, the observed changes in fiber type composition cannot be explained

Development (2016) 143, 1547-1559 doi:10.1242/dev.129676

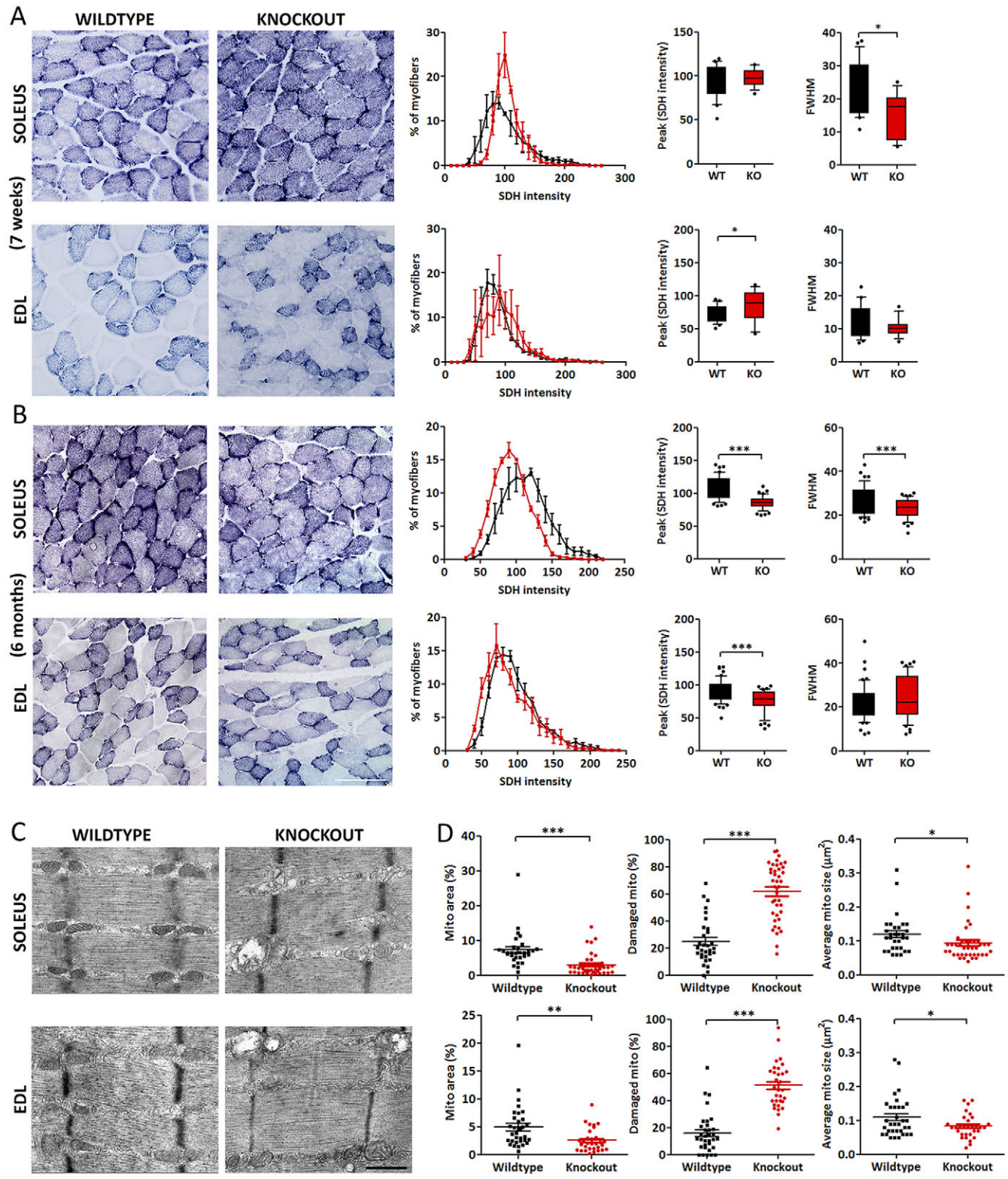

Fig. 6. Mitochondrial content and enzyme activity are reduced in $Ca_V1.1^{\Delta E29/\Delta E29}$ muscles. (A,B) SDH activity was analyzed in sections of wild-type (black) and $Ca_V1.1^{\Delta E29/\Delta E29}$ (red) mice. Staining intensity was measured in each fiber profile and plotted in intensity distribution diagrams. (A) In 7-week-old mice, SDH activity is markedly increased in $Ca_V1.1^{\Delta E29/\Delta E29}$ soleus and EDL muscles, as seen by the right-shifted intensity distribution histogram. (B) In 6-month-old mice, SDH activity is significantly reduced in $Ca_V1.1^{\Delta E29/\Delta E29}$ soleus muscle and in EDL muscles. In EDL also the full width at half maximum (FWHM) was reduced. *N*=3. (C) Electron micrographs of 4- and 5-month-old wild-type and $Ca_V1.1^{\Delta E29/\Delta E29}$ soleus and EDL muscles. Whereas myofibrils and EC coupling membranes appear normal, dilated and lysed mitochondria are found in $Ca_V1.1^{\Delta E29/\Delta E29}$ muscles. (D) Morphometric analysis demonstrates significantly decreased fractional content (percentage area occupied by intact mitochondria) in both $Ca_V1.1^{\Delta E29/\Delta E29}$ muscle types. Mitochondrial size is decreased in $Ca_V1.1^{\Delta E29/\Delta E29}$ muscles and the fraction of damaged mitochondria increased in $Ca_V1.1^{\Delta E29/\Delta E29}$ soleus muscles. *N*=30-40 images of two biological replicates per condition. **P*<0.05, ***P*<0.01, ****P*<0.001. Mean±s.e.m. See also Fig. S3. Scale bars: 100 µm in A,B; 0.5 µm in C.

Development (2016) 143, 1547-1559 doi:10.1242/dev.129676

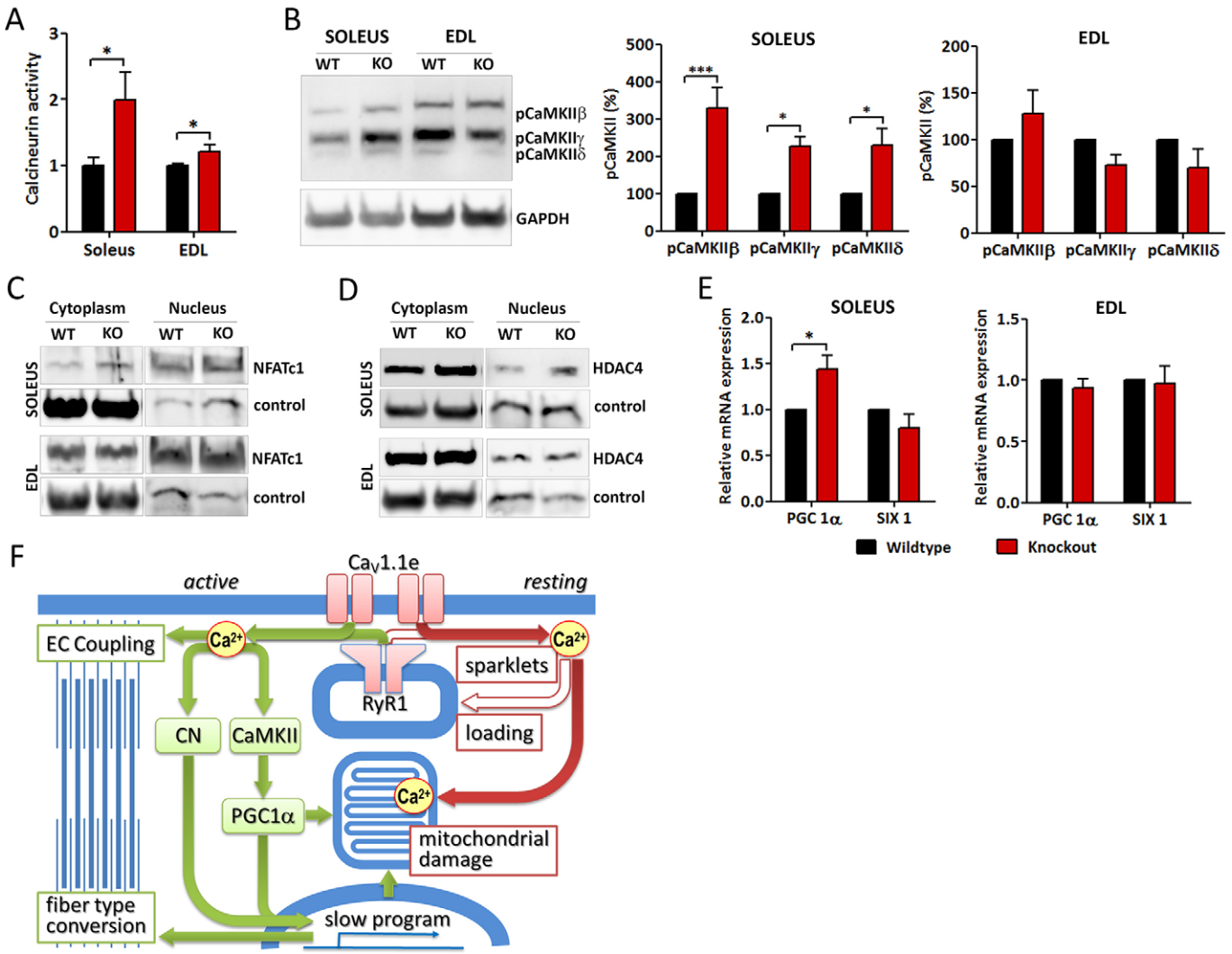

Fig. 7. Altered expression of regulators of fiber type specification and mitochondrial biogenesis in slow and fast muscles of $Ca_V1.1^{\Delta E29/\Delta E29}$ mice. (A) Basal enzymatic activity of calcineurin is significantly increased in $Ca_V1.1^{\Delta E29/\Delta E29}$ soleus and EDL muscles (red) compared with wild type (black). (B) Western blot analysis shows a significant increase of activated CaMKII β, γ and δ isoforms (phosphorylated at Thr286) in soleus but not EDL muscle of $Ca_V1.1^{\Delta E29/\Delta E29}$. (C,D) Cytoplasmic and nuclear localization of NFATC1 and HDAC4 does not differ between the genotypes (age of mice 6-8 months). Controls for the cytoplasm and nuclear fraction are GAPDH and histone H3, respectively. *N*=3. (E) Quantitative RT-PCR analysis demonstrates that expression of *PGC1α* (*Ppargc1a*) mRNA is significantly increased in $Ca_V1.1^{\Delta E29/\Delta E29}$ soleus muscles, whereas the decline of *PGC1α* in EDL and of *Six1* expression in both muscles is not significant. *N*=3. **P*<0.05, ****P*<0.001. Mean±s.e.m. (F) Model of signaling pathways causing fiber type shift and mitochondrial damage in $Ca_V1.1^{\Delta E29/\Delta E29}$ muscles. During EC coupling, increased calcium influx through Ca$_V$1.1e activates calcineurin (CN), CaMKII and PGC1α, the primary regulators of fiber type specification and mitochondrial biogenesis. The shift in fiber type composition in the slow direction offsets the direct effects of increased calcium signals on EC coupling. Parallel upregulation of oxidative metabolism by PGC1α is counteracted by mitochondrial damage caused by calcium overload due to increased activity-dependent and spontaneous calcium influx and altered calcium homeostasis. See also Fig. S4.

as a normal adaptive response to altered activity, but represent a dysregulation of fiber type composition owing to the absence of postnatal inclusion of *Ca$_V$1.1* exon 29 in $Ca_V1.1^{\Delta E29/\Delta E29}$ mice. Since Ca$_V$1.1 is almost exclusively expressed in skeletal muscle and the functional effects (e.g. reduced force, increased fatigue resistance) were observed in isolated muscles, muscle-intrinsic mechanisms are likely to be responsible for the altered muscle fiber type composition in $Ca_V1.1^{\Delta E29/\Delta E29}$ mice.

Expression of Ca$_V$1.1e alters skeletal muscle calcium signaling and activates the pathways for the slow twitch fiber program

Calcium is the principal second messenger regulating adaptive changes of muscle properties in response to training or experimentally altered innervation patterns (Bassel-Duby and Olson, 2006; Chin et al., 1998; Liu et al., 2005). As the primary defects in the $Ca_V1.1^{\Delta E29/\Delta E29}$ mice are altered gating and conduction properties of the skeletal muscle L-type calcium channel expressed in adult mice, a role of increased calcium influx in determining the fiber type composition is very likely. In cultured dysgenic myotubes reconstituted with either of two Ca$_V$1.1 splice variants, we previously reported that exclusion of exon 29 caused a 30 mV left-shifted voltage dependence of current activation and an 8-fold increase in current density (Tuluc et al., 2009). Here, we demonstrate that also in isolated muscle fibers of $Ca_V1.1^{\Delta E29/\Delta E29}$ mice, sole expression of the Ca$_V$1.1e splice variant causes an equally large left shift of voltage sensitivity and a substantially increased calcium influx during EC coupling. Interestingly, the calcium influx on top of the calcium released from the SR was not reflected in a parallel increase in contractile

Development (2016) 143, 1547-1559 doi:10.1242/dev.129676

strength. This indicates that, with respect to muscle contraction, the effects of increased calcium influx are counteracted by other consequences of the altered calcium signaling in $Ca_V1.1^{\Delta E29/\Delta E29}$ mice. In fact, the observed fiber type shift to slower, and thus weaker, fiber types could be part of a compensatory response of the muscle cell to an increased calcium load during EC coupling. The effects of continued expression of the calcium-conducting $Ca_V1.1e$ splice variant on fatigability and fiber type composition are consistent with recently published results obtained in a *$Ca_V1.1$* mutant (Lee et al., 2015). A knock-in mouse with a mutation in the $Ca_V1.1$ pore that abolished calcium binding and conduction showed increased fatigability and type IIB fiber content. Together, the two studies demonstrate that fiber type specification in skeletal muscle is highly sensitive to the magnitude of L-type calcium currents. The loss of calcium influx through $Ca_V1.1$ shifts the muscles towards a faster phenotype, whereas an increase of calcium currents causes a shift towards a slower phenotype.

In addition to altered calcium transients during EC coupling, a nisoldipine-sensitive component of calcium influx was observed in a store-refilling protocol, indicating that the extra calcium influx through the developmental $Ca_V1.1e$ splice variant also contributes to mechanisms of calcium homeostasis. Functionally, increased store filling probably contributes to the increased fatigue resistance observed in muscles of $Ca_V1.1^{\Delta E29/\Delta E29}$mice. Consistent with this notion, the opposite effects – decreased store filling and decreased fatigue resistance – were observed in the calcium permeation mutant mouse (Lee et al., 2015).

Furthermore, at rest muscle fibers of $Ca_V1.1^{\Delta E29/\Delta E29}$ mice generated focal calcium transients – so called calcium sparklets. Although calcium sparks are common in cardiac muscle cells, in developing skeletal muscle fibers and in cultured myotubes, they have never before been observed in mature muscle fibers of healthy mice (Cheng and Lederer, 2008; Weisleder and Ma, 2006). The calcium sparklets observed in $Ca_V1.1^{\Delta E29/\Delta E29}$ mice were dependent on the extracellular calcium concentration and were sensitive to the L-type channel blocker nisoldipine. Thus, there can be little doubt that calcium influx through $Ca_V1.1e$ channels contributed directly or indirectly to this phenomenon. As calcium sparks in cardiac myocytes can be activated by the opening of even a single $Ca_V1.2$ channel (Lopez-Lopez et al., 1995), it is conceivable that in skeletal muscles spontaneous openings of $Ca_V1.1e$ channels trigger the opening of RyR1 and thus activate calcium sparklets by calcium-induced calcium release. In wild-type mice this is limited to developing myotubes, which naturally express the $Ca_V1.1e$ splice variant. In $Ca_V1.1^{\Delta E29/\Delta E29}$ mice these spontaneous calcium signals occur also in differentiated muscles, where they might affect signaling pathways regulating fiber type composition and cause mitochondrial damage.

Downstream of calcium, it is calcineurin and CaMKII that are the key regulators of fast to slow twitch fiber type changes (Chin et al., 1998). Calcineurin regulates transcription of muscle genes via the classical NFAT pathway, CaMKII via HDAC4. Both converge on MEF2, but have also been reported to activate PGC1α (Tavi and Westerblad, 2011). A key feature of these parallel signaling pathways is their ability to distinguish between calcium signals in response to chronic, repetitive (slow fiber type) activation patterns and those in response to phasic (fast fiber type) activation patterns (Liu et al., 2005; Tavi and Westerblad, 2011). Apparently, expression of a calcium-conducting $Ca_V1.1e$ splice variant in adult muscles tips the balance of this delicate calcium sensing mechanism and leads to constitutive activation of the signaling pathway for the slow muscle program (Fig. 7F). Consistent with this notion, we observed that calcineurin and CaMKII activity, as well as expression of PGC1α, were constitutively upregulated in skeletal muscles of $Ca_V1.1^{\Delta E29/\Delta E29}$ mice, and that activation of CaMKII and PGC1α was specific to slow muscles. In accordance with this, altered CaMKII signaling was also observed in the calcium permeation *$Ca_V1.1$* mutant (Lee et al., 2015).

Thus, in $Ca_V1.1^{\Delta E29/\Delta E29}$ mice the continuous expression of $Ca_V1.1e$ causes increased calcium influx during EC coupling, in homeostatic calcium regulation, and at rest. Which of these calcium influx events contribute to the activation of the slow muscle pathway remains to be determined. Because calcineurin and CaMKII signaling is highly sensitive to the calcium signaling patterns in response to slow fiber type-specific activity, we favor a role of altered calcium signal during EC coupling. In any case, if aberrant activation of these signaling pathways causes an increase in slow fibers in $Ca_V1.1^{\Delta E29/\Delta E29}$ mice, during normal development the alternative splicing event causing the shift from a calcium-conducting to a non-conducting $Ca_V1.1$ variant might be an important prerequisite for the proper regulation of fiber type composition at basal activity levels as well as in response to exercise.

The contribution of aberrant $Ca_V1.1$ splicing to myotonic dystrophy

Splicing defects of important muscle proteins, including the CLCN1 chloride channel, insulin receptor, SERCA1 (ATP2A1) and $Ca_V1.1$, lead to DM1 (Thornton, 2014). The myotonia is likely to be caused by a hyperexcitability of muscles due to the loss of CLCN1 function (Lueck et al., 2007). Because aberrant expression of the $Ca_V1.1e$ splice variant correlates with the degree of muscle weakness in DM1 patients, and forced missplicing of *$Ca_V1.1$* exon 29 caused centrally localized nuclei in a myotonia mouse model, it has been suggested that increased calcium influx through the developmental $Ca_V1.1e$ splice variant may contribute to the myopathy (Santoro et al., 2014; Tang et al., 2012). This hypothesis is in line with the known role of increased calcium influx via various entry pathways in muscular dystrophy (Allen et al., 2010; Whitehead et al., 2006). Here, we examined whether aberrant missplicing of *$Ca_V1.1$* exon 29 by itself is sufficient to cause DM-like symptoms. At the organismal level this was not the case. Homozygous $Ca_V1.1^{\Delta E29/\Delta E29}$ mice, which exclusively express the developmental $Ca_V1.1e$ splice variant, did not show severe muscle weakness, and their muscle sections did not reveal centrally located nuclei, which is a histopathological hallmark of dystrophic muscle. Although the contractile force of isolated muscles was reduced, this was accompanied by increased fatigue resistance and might therefore be the consequence of the fiber type shift rather than a symptom of DM1.

We observed decreased SDH activity and severe mitochondrial damage in muscles of mature and aged $Ca_V1.1^{\Delta E29/\Delta E29}$ mice. Similar mitochondrial damage has been described in other mouse muscle disease models with aberrant calcium signaling (Irwin et al., 2003). Calcium overload leads to mitochondrial damage and ultimately produces the symptomatic central cores in the diseased muscles (Boncompagni et al., 2009; Brookes et al., 2004). Similarly, the $Ca_V1.1e$-mediated spontaneous calcium sparklets, or the increased calcium influx after store depletion, might overburden the mitochondrial calcium handling capacity and cause their loss in $Ca_V1.1^{\Delta E29/\Delta E29}$ muscles. In fact, both calcium sparks and store-operated calcium currents have previously been implicated in the pathophysiology of muscular dystrophy (Goonasekera et al., 2014; Weisleder and Ma, 2006). Thus, the mitochondrial damage observed in $Ca_V1.1^{\Delta E29/\Delta E29}$ mice might precede the appearance of histopathological and clinical features of DM1.

Development (2016) 143, 1547-1559 doi:10.1242/dev.129676

We conclude that, by itself, missplicing of exon 29 in *$Ca_V1.1$* is not sufficient to reproduce the full spectrum of DM1 symptoms in mice. As the disease phenotype in dystrophy and myotonia mouse models is often less severe than in human disease, this does not preclude the possibility that missplicing of $Ca_V1.1$ makes a notable contribution to the disease in DM1 patients. Furthermore, it is likely that in combination with the splicing defects in other muscle genes involved in calcium handling (*Serca1*) and excitability (*Clcn1*), the mitochondrial damage observed in the *$Ca_V1.1^{\Delta E29/\Delta E29}$* mice might be aggravated, and thus contribute to the myopathy (Tang et al., 2012). If so, the use of clinically approved L-type calcium channel blockers to target $Ca_V1.1e$ currents might be a viable strategy to alleviate the symptoms of DM1 (Benedetti et al., 2015).

In conclusion, the effects of $Ca_V1.1$ missplicing in the *$Ca_V1.1^{\Delta E29/\Delta E29}$* mice revealed a novel role of increased L-type calcium currents in the dysregulation of muscle fiber type composition. With regard to normal muscle physiology these findings suggest that, during development, skeletal muscles actively suppress L-type calcium currents by alternative splicing of $Ca_V1.1$, so as to prevent unrestrained calcium influx during EC coupling from interfering with the second calcium signaling function in regulating muscle fiber type composition. Furthermore, aberrant expression of the developmental $Ca_V1.1e$ splice variant in mature muscles causes mitochondrial damage, which might contribute to the pathology of DM1.

MATERIALS AND METHODS

Mice and animal care

$Ca_V1.1^{\Delta E29}$ mice were generated in a C57BL/6N background at Taconic Artemis (Cologne, Germany). All experimental protocols conformed to guidelines of the European Community (86/609/EEC) and were approved by the Austrian Ministry of Science (BMWF-66.011/0069-II/10b/2010) and by the Institutional Animal Care Committee of the University of Debrecen (22/2011/DE MAB). Genotyping is described in the supplementary Materials and Methods.

Quantitative RT-PCR

RNA was isolated from muscles of wild-type and *$Ca_V1.1^{\Delta E29}$* mice using the RNeasy Fibrous Tissue Mini Kit (Qiagen). After reverse transcription (SuperScript II reverse transcriptase, Invitrogen) the absolute number of transcripts was assessed by quantitative TaqMan PCR (50 cycles). For primer sequences and experimental details, see the supplementary Materials and Methods and Table S1.

Microarray

Affymetrix GeneChip analysis of mRNA expression in soleus and EDL muscles of wild-type and *$Ca_V1.1^{\Delta E29/\Delta E29}$* mice was performed as detailed in the supplementary Materials and Methods.

Behavioral experiments

The following tests were performed on 2- and 8-month-old wild-type, heterozygous *$Ca_V1.1^{+/\Delta E29}$* and homozygous *$Ca_V1.1^{\Delta E29/\Delta E29}$* mice: home cage activity, voluntary running, Rotarod test, wire hang test, grip force measurements. For details, see the supplementary Materials and Methods.

Force measurements

Contractile force of isolated EDL and soleus muscles of 3- to 6-month-old mice in response to twitch and tetanic stimulations were recorded with a capacitative mechanoelectric force transducer as described in the supplementary Materials and Methods.

Single fiber measurements

Single fibers were isolated from FDB muscles and used for voltage-clamp recordings of calcium currents with an Axoclamp 2B amplifier (Axon Instruments), and cytoplasmic calcium signals were recorded using fluorescent calcium indicators and imaging with a Zeiss 5 Live confocal microscope (20× objective). Further experimental details and data analysis are described in the supplementary Materials and Methods.

Immunohistochemistry and SDH activity assay

Cryosections of EDL and soleus muscles from 6-month-old wild-type and *$Ca_V1.1^{\Delta E29/\Delta E29}$* mice were immunostained with antibodies against specific myosin heavy chain isoforms (Developmental Studies Hybridoma Bank, University of Iowa, Iowa, USA). Histochemical staining of SDH activity was performed with succinic acid and nitroblue tetrazolium for 1 h. For information on the antibodies used and further details of experimental and quantification procedures, see the supplementary Materials and Methods and Table S2.

Western blot and calcineurin assay

Cytoplasmic and nuclear protein fractions were prepared from 6-month-old wild-type and *$Ca_V1.1^{\Delta E29/\Delta E29}$* mice and separated on 6-10% bis-Tris gels for western blotting. Calcineurin activity was determined using a Calcineurin Phosphatase Activity Colorimetric Assay (Abcam) according to the manufacturer's instructions. For antibodies and experimental details, see the supplementary Materials and Methods.

Electron microscopy

Tissue processing for transmission electron microscopy of EDL and soleus muscles, and the analysis of mitochondria, were performed as detailed in the supplementary Materials and Methods.

Statistical analysis

A two-way ANOVA with Bonferroni post-hoc test was used for home cage activity and fiber type analysis. One-way ANOVA was used for the other behavioral tests. Student's *t*-test and Mann–Whitney U-test were used to calculate the statistical significance for fiber type and contractile properties analysis. *N* represents the number of animals. Data are presented as mean± s.e.m. The statistical analysis was performed with GraphPad Prism. For further details see the supplementary Materials and Methods.

Acknowledgements

We thank Dr C. Humpel for providing muscle samples of aged mice; Dr S. Schiaffino for helpful advice on fiber type analysis; Dr B. Lontay for assistance with calcineurin activity measurements; and R. Őri, K. Gutleben and B. Witting for excellent technical assistance.

Competing interests

The authors declare no competing or financial interests.

Author contributions

B.E.F., N.S. and L.C. designed research and wrote the manuscript. N.S., B.D., A.B., P.T., P.S., M.S., J.R., M.W.H., C.S. and G.J.O. performed experiments and/or analyzed data.

Funding

This work was supported by grants from the Austrian Science Fund (FWF) [P23479 and W1101] to B.E.F.; from the Hungarian Scientific Research Fund (OTKA) [NN-107765]; from the European Union and the State of Hungary, co-financed by the European Social Fund in the framework of TÁMOP-4.1.2.E-13/1/KONV-2013-0010 and TÁMOP-4.2.4.A/2-11/1-2012-0001 'National Excellence Program' to B.D. Deposited in PMC for immediate release.

Data availability

The raw and preprocessed microarray data are available at Gene Expression Omnibus under accession number GSE67803.

Supplementary information

Supplementary information available online at
http://dev.biologists.org/lookup/suppl/doi:10.1242/dev.129676/-/DC1

References

Allen, D. L., Harrison, B. C., Maass, A., Bell, M. L., Byrnes, W. C. and Leinwand, L. A. (2001). Cardiac and skeletal muscle adaptations to voluntary wheel running in the mouse. *J. Appl. Physiol.* **90**, 1900-1908.

Allen, D. G., Gervasio, O. L., Yeung, E. W. and Whitehead, N. P. (2010). Calcium and the damage pathways in muscular dystrophy. *Can. J. Physiol. Pharmacol.* **88**, 83-91.

Bassel-Duby, R. and Olson, E. N. (2006). Signaling pathways in skeletal muscle remodeling. *Annu. Rev. Biochem.* **75**, 19-37.
Benedetti, B., Tuluc, P., Mastrolia, V., Dlaska, C. and Flucher, B. E. (2015). Physiological and pharmacological modulation of the embryonic skeletal muscle calcium channel splice variant CaV1.1e. *Biophys. J.* **108**, 1072-1080.
Boncompagni, S., Rossi, A. E., Micaroni, M., Hamilton, S. L., Dirksen, R. T., Franzini-Armstrong, C. and Protasi, F. (2009). Characterization and temporal development of cores in a mouse model of malignant hyperthermia. *Proc. Natl. Acad. Sci. USA* **106**, 21996-22001.
Brookes, P. S., Yoon, Y., Robotham, J. L., Anders, M. W. and Sheu, S.-S. (2004). Calcium, ATP, and ROS: a mitochondrial love-hate triangle. *Am. J. Physiol. Cell Physiol.* **287**, C817-C833.
Cheng, H. and Lederer, W. J. (2008). Calcium sparks. *Physiol. Rev.* **88**, 1491-1545.
Chin, E. R. (2005). Role of Ca2+/calmodulin-dependent kinases in skeletal muscle plasticity. *J. Appl. Physiol.* **99**, 414-423.
Chin, E. R., Olson, E. N., Richardson, J. A., Yang, Q., Humphries, C., Shelton, J. M., Wu, H., Zhu, W., Bassel-Duby, R. and Williams, R. S. (1998). A calcineurin-dependent transcriptional pathway controls skeletal muscle fiber type. *Genes Dev.* **12**, 2499-2509.
Flucher, B. E. and Tuluc, P. (2011). A new L-type calcium channel isoform required for normal patterning of the developing neuromuscular junction. *Channels* **5**, 518-524.
Gomes-Pereira, M., Cooper, T. A. and Gourdon, G. (2011). Myotonic dystrophy mouse models: towards rational therapy development. *Trends Mol. Med.* **17**, 506-517.
Goonasekera, S. A., Davis, J., Kwong, J. Q., Accornero, F., Wei-LaPierre, L., Sargent, M. A., Dirksen, R. T. and Molkentin, J. D. (2014). Enhanced Ca(2)(+) influx from STIM1-Orai1 induces muscle pathology in mouse models of muscular dystrophy. *Hum. Mol. Genet.* **23**, 3706-3715.
Grifone, R., Laclef, C., Spitz, F., Lopez, S., Demignon, J., Guidotti, J.-E., Kawakami, K., Xu, P.-X., Kelly, R., Petrof, B. J. et al. (2004). Six1 and Eya1 expression can reprogram adult muscle from the slow-twitch phenotype into the fast-twitch phenotype. *Mol. Cell. Biol.* **24**, 6253-6267.
Handschin, C., Chin, S., Li, P., Liu, F., Maratos-Flier, E., LeBrasseur, N. K., Yan, Z. and Spiegelman, B. M. (2007). Skeletal muscle fiber-type switching, exercise intolerance, and myopathy in PGC-1alpha muscle-specific knock-out animals. *J. Biol. Chem.* **282**, 30014-30021.
Irwin, W. A., Bergamin, N., Sabatelli, P., Reggiani, C., Megighian, A., Merlini, L., Braghetta, P., Columbaro, M., Volpin, D., Bressan, G. M. et al. (2003). Mitochondrial dysfunction and apoptosis in myopathic mice with collagen VI deficiency. *Nat. Genet.* **35**, 367-371.
Krüger, K., Gessner, D. K., Seimetz, M., Banisch, J., Ringseis, R., Eder, K., Weissmann, N. and Mooren, F. C. (2013). Functional and muscular adaptations in an experimental model for isometric strength training in mice. *PLoS ONE* **8**, e79069.
Lee, C. S., Dagnino-Acosta, A., Yarotskyy, V., Hanna, A., Lyfenko, A., Knoblauch, M., Georgiou, D. K., Poché, R. A., Swank, M. W., Long, C. et al. (2015). Ca(2+) permeation and/or binding to CaV1.1 fine-tunes skeletal muscle Ca(2+) signaling to sustain muscle function. *Skeletal Muscle* **5**, 4.
Lin, J., Wu, H., Tarr, P. T., Zhang, C.-Y., Wu, Z., Boss, O., Michael, L. F., Puigserver, P., Isotani, E., Olson, E. N. et al. (2002). Transcriptional co-activator PGC-1 alpha drives the formation of slow-twitch muscle fibres. *Nature* **418**, 797-801.
Liu, Y., Randall, W. R. and Schneider, M. F. (2005). Activity-dependent and -independent nuclear fluxes of HDAC4 mediated by different kinases in adult skeletal muscle. *J. Cell Biol.* **168**, 887-897.
Lopez-Lopez, J. R., Shacklock, P. S., Balke, C. W. and Wier, W. G. (1995). Local calcium transients triggered by single L-type calcium channel currents in cardiac cells. *Science* **268**, 1042-1045.
Lueck, J. D., Mankodi, A., Swanson, M. S., Thornton, C. A. and Dirksen, R. T. (2007). Muscle chloride channel dysfunction in two mouse models of myotonic dystrophy. *J. Gen. Physiol.* **129**, 79-94.
Melzer, W., Herrmann-Frank, A. and Lüttgau, H. C. (1995). The role of Ca2+ ions in excitation-contraction coupling of skeletal muscle fibres. *Biochim. Biophys. Acta* **1241**, 59-116.
Rodríguez, E. G., Lefebvre, R., Bodnár, D., Legrand, C., Szentesi, P., Vincze, J., Poulard, K., Bertrand-Michel, J., Csernoch, L., Buj-Bello, A. et al. (2014). Phosphoinositide substrates of myotubularin affect voltage-activated Ca(2)(+) release in skeletal muscle. *Pflugers Arch.* **466**, 973-985.
Santoro, M., Piacentini, R., Masciullo, M., Bianchi, M. L. E., Modoni, A., Podda, M. V., Ricci, E., Silvestri, G. and Grassi, C. (2014). Alternative splicing alterations of Ca2+ handling genes are associated with Ca2+ signal dysregulation in myotonic dystrophy type 1 (DM1) and type 2 (DM2) myotubes. *Neuropathol. Appl. Neurobiol.* **40**, 464-476.
Szentesi, P., Jacquemond, V., Kovács, L. and Csernoch, L. (1997). Intramembrane charge movement and sarcoplasmic calcium release in enzymatically isolated mammalian skeletal muscle fibres. *J. Physiol.* **505**, 371-384.
Tang, Z. Z., Yarotskyy, V., Wei, L., Sobczak, K., Nakamori, M., Eichinger, K., Moxley, R. T., Dirksen, R. T. and Thornton, C. A. (2012). Muscle weakness in myotonic dystrophy associated with misregulated splicing and altered gating of Ca (V)1.1 calcium channel. *Hum. Mol. Genet.* **21**, 1312-1324.
Tavi, P. and Westerblad, H. (2011). The role of in vivo Ca(2)(+) signals acting on Ca (2)(+)-calmodulin-dependent proteins for skeletal muscle plasticity. *J. Physiol.* **589**, 5021-5031.
Thornton, C. A. (2014). Myotonic dystrophy. *Neurol. Clin.* **32**, 705-719, viii.
Tuluc, P., Molenda, N., Schlick, B., Obermair, G. J., Flucher, B. E. and Jurkat-Rott, K. (2009). A CaV1.1 Ca2+ channel splice variant with high conductance and voltage-sensitivity alters EC coupling in developing skeletal muscle. *Biophys. J.* **96**, 35-44.
Weisleder, N. and Ma, J.-j. (2006). Ca2+ sparks as a plastic signal for skeletal muscle health, aging, and dystrophy. *Acta Pharmacol. Sin.* **27**, 791-798.
Whitehead, N. P., Yeung, E. W. and Allen, D. G. (2006). Muscle damage in mdx (dystrophic) mice: role of calcium and reactive oxygen species. *Clin. Exp. Pharmacol. Physiol.* **33**, 657-662.
Wu, H., Rothermel, B., Kanatous, S., Rosenberg, P., Naya, F. J., Shelton, J. M., Hutcheson, K. A., DiMaio, J. M., Olson, E. N., Bassel-Duby, R. et al. (2001). Activation of MEF2 by muscle activity is mediated through a calcineurin-dependent pathway. *EMBO J.* **20**, 6414-6423.
Wu, W., Ren, Z., Zhang, L., Liu, Y., Li, H. and Xiong, Y. (2013). Overexpression of Six1 gene suppresses proliferation and enhances expression of fast-type muscle genes in C2C12 myoblasts. *Mol. Cell. Biochem.* **380**, 23-32.

Supplementary Materials and Methods:

Genotyping

Genomic DNA was isolated from ear punches or tail biopsies of mice using the HOTSHOT method as described previously (Truett et al., 2000). The PCR conditions for genotyping: 95°C for 3 min, 95°C for 30 sec, 60°C for 30 sec, 72°C for 40 sec, repeated for 30 cycles; 72°C for 5 min. The forward primer and the reverse primers for the $Ca_V1.1$ gene were 5´ -CCTGTCTCTGTCTGGTCTTCC- 3´ and 5´ -GCCTGCTCTAAGGAAAGGAG- 3´, respectively. Expected band size for $Ca_V1.1\Delta E29$ is 344 bp and for wildtype is 373 bp.

Quantitative TaqMan RT-PCR

For expression analysis of $Ca_V1.1$ splice variants RNA was isolated from soleus (Sol), extensor digitorum longus (EDL) and diaphragm (Dia) muscle of E17, newborn, 3 weeks, 6 weeks, 16 weeks and 15-18 months old mice using the RNeasy® Fibrous Tissue Mini kit (Qiagen, Cat. No.74704, Venlo, NL). Except for the 15-18 months old mice, in which case only wildtype males were used, muscles were isolated from mice of either sex and of all genotypes. Following reverse transcription (SuperScript®II Reverse Transcriptase, Invitrogen, Carlsbad, CA, USA), the absolute number of $Ca_V1.1a$ and $Ca_V1.1e$ transcripts was assessed by quantitative TaqMan PCR (50 cycles), using a standard curve generated from PCR products of known concentrations as described previously (Schlick et al., 2010). For primers see Supplementary Table 1.

To analyze expression of other genes involved in fiber type regulation, only Sol and EDL muscles were used from 6-7 months old mice. The relative mRNA expression levels of PGC-1α and SIX1 were calculated as relative amount of specific cDNA versus HPRT1, using the ΔΔCt method ($2^{-\Delta\Delta Ct}$), where ΔCt was defined as Ct (gene) – Ct (HPRT1, housekeeping gene) and ΔΔCt as ΔCt – ΔCt (WT control). Taqman gene expression assays designed to span exon-exon boundaries (Table S1) were purchased from Applied Biosystems (Vienna, AT). Data were normalized as described previously (Schlick et al., 2010) and analyzed using the ABI PRISM 7500 sequence detector (Applied Biosystems, Vienna, AT).

Affymetrix GeneChip analysis

The whole-genome gene expression data were obtained at the Expression Profiling Unit of the Medical University Innsbruck using the Affymetrix GeneChip MoGene-1.0-ST-v1 Array. Sample

preparation was performed according to the manufacturer's protocols. In brief, RNA quantity and purity was determined by optical density measurements (OD 260/280 ratio) and by measuring the RNA integrity using the Agilent Technologies 2100 Bioanalyzer. Then, 250 ng of RNA per sample were processed to generate biotinylated hybridization targets using the Affymetrix GeneChip WT Expression kit and the Affymetrix GeneChip WT Terminal Labeling KIR. Resulting targets were hybridized to the Affymetrix GeneChip MoGene-1.0 ST v1 and stained in an Affymetrix fluidic station 450. Raw fluorescence signal intensities were recorded by an Affymetrix scanner 3000 and image analysis was performed with the Affymetrix GeneChip Command Console software (AGCC). All further analysis was performed in R (version 3.1.2) using packages from the Bioconductor project (Gentleman et al., 2004). Pre-processing of the raw microarray data was performed as described in (Bindreither et al., 2014). In brief, raw microarray data was pre-processed using the "generalgcrma" package (Rainer et al., 2012) and our custom transcript-level "CEL definition file" (CDF) that defines probe sets for each transcript of all genes in the Ensembl database version 75. After GCRMA pre-processing a representative transcript probe set was selected for each gene based on a combination of its average expression and variance of expression across all EDL or Soleus samples.

Differential gene expression analysis was performed using the limma package (Smyth, 2004). The resulting p-values were subsequently adjusted for multiple hypothesis testing using the method from Benjamini and Hochberg (Benjamini and Hochberg, 1995) for a strong control of the false discovery rate (FDR). Genes with an M-value > 1 (representing more than 2-fold regulation) at a 5% FDR (adjusted p-value < 0.05) were considered to be significantly differentially expressed.

The raw and preprocessed microarray data have been submitted to the Gene Expression Omnibus (http://www.ncbi.nlm.nih.gov/geo/query/acc.cgi?token=shkxmwesffehzcb&acc=GSE67803).

Behavioral experiments

All behavioral experiments were done at 2 and 8 months of age.

Wire hang test: Mice were put on a wire mesh which was then turned upside down. Time was recorded until the mice fell off, or tests were ended at 60 s. Tests were repeated thrice for each mouse.

Homecage activity: To monitor the homecage activity, mice were individually placed in cages with free access to food and water, enriched with a plastic tube. Movement of mice was monitored through an infrared detection system (InfraMot, TSE Systems, Homburg, DE). Analysis was started at

5 PM for a 72 h period. Arbitrary activity counts for a period of 48 h starting from 6:46 AM were collapsed into 60 min bins to examine the hourly distribution of activity.

Rotarod test: The mice had two familiarization trials on the rotarod (Acceler Rota-Rod 7650, Ugo Basile, IT) at 4 rpm for 1 min each with an interval of 10 min between the trials. 30 min after the second familiarization trial, they were tested on an accelerating (4-40 rpm) rotarod for up to 300 s. The test was repeated after 15 min.

Treadmill: The mice were familiarized to the treadmill (Exer 3/6 open treadmill, Columbus Instruments, Ohio, USA) for 30 min at rest followed by two times for 5 min at a speed of 10 m/min at an interval of 5 min. The next day before starting the test, the mice underwent another familiarization for 5 min at 10m/min. 15 min after this familiarization the mice were tested with an accelerating speed starting at 10 m/min increasing for 2 m/min every 5 min. The cut off time was 30 min.

Voluntary activity wheel measurement: Mice from both groups were singly housed in a cage with a mouse running wheel (Campden Instruments Ltd., Loughborough, UK). Wheels were interfaced to a computer and revolutions were recorded in 20 minutes intervals, continuously for 8 days. The average and the maximal speed, the distance and the duration of running was calculated for the individual mice and then averaged by groups.

Forepaw grip test: The force of forepaw was measured as described earlier (Bodnar et al., 2014). Briefly, when the animals reliably grasped the bar of the grip test meter, they were then gently pulled away from the device. The maximal force before the animal released the bar were digitized at 2 kHz and stored by an online connected computer. For better comparison the maximal force was normalized to the body weight of the animals.

Measurement of contractile force

Muscle contractions of 3-6 month old mice were measured as described previously (Oddoux et al., 2009). In brief, EDL and Sol were placed horizontally in an experimental chamber continuously superfused (10 ml/min) with Krebs' solution (containing in mM: NaCl 135, KCl 5, $CaCl_2$ 2.5, $MgSO_4$ 1, Hepes 10, glucose 10, $NaHCO_3$ 10; pH 7.2; room temperature) equilibrated with 95% O_2 plus 5% CO_2. One end of the muscle was attached to a rod, the other to a capacitive mechanoelectric force transducer. Contractions were elicited by 2 ms supramaximal electrical pulses delivered by two platinum electrodes placed adjacent to the muscle. Force responses were digitized at 2 kHz by using Digidata 1200 A/D card and acquired with Axotape software (Axon Instruments, Foster City, CA,

USA). Muscles were then stretched by adjusting the position of the transducer to a length that produced the maximal force response and allowed to equilibrate for 60 min before testing. At least 10 twitches at 2 s intervals were recorded from each muscle. The individual force transients within such a train varied by less than 3% in amplitude, thus the mean of the amplitude of all transients was used to characterize the given muscle. To elicit tetanic contractions, trains of pulses were applied with a frequency of 200 Hz for 200 ms (EDL) or 100 Hz for 500 ms (Sol). Duration of individual twitches and tetani were determined by calculating the time between the onset of the transient and the relaxation to 90% of maximal force. The time constant (Tau) of the On and Off phase of contraction was determined from a single exponential fit to the rising and falling phase of the force transient. To test muscles fatigue 150 tetani were applied with 0.5 Hz (Oddoux et al., 2009). The degree of fatigue was expressed by normalizing the amplitude of each tetanus to that of the first tetanus. The tetanic fusion frequency was tested with a series of repeated pulses stimulated at increasing frequencies starting from 10 Hz. To quantify development of complete tetanus the following equation was fitted to the maximum of the force transient in one series:

$$T = A/(1+\exp(-(F-F_{50})/k) \qquad \text{(Eqn. 1.)}$$

where T is the actual tension at frequency F, A is the amplitude of the maximal tetanus, F_{50} is the frequency at half maximal tension and k is the slope factor of the function.

Isolation of whole skeletal muscles and single muscle fibers

3-4 month old mice were anesthesied with pentobarbital (27 mg/kg), then *m. flexor digitorum brevis* (FDB) from the fore limb, and the EDL and Sol from the hind limb were dissected. Single muscle fibers were enzymatically dissociated in calcium free modified Tyrode's solution (in mM, 137 NaCl, 5.4 KCl, 0.5 MgCl2, 11.8 Hepes, pH 7.4) containing 0.2% Type I collagenase (Sigma, St. Louis, USA) at 37°C for 50-55 minutes (Csernoch et al., 2008). To release single fibers muscles were triturated gently in modified Tyrode's solution supplemented with 1.8 mM $CaCl_2$. The fibers were then mounted on laminin-coated cover slip floors of culture dishes and kept at 4°C until use.

Voltage clamp and I_{Ca} measurement

The experimental design was as described in (Sztretye et al., 2011). Briefly, isolated fibers were voltage-clamped (Axoclamp 2B, Axon Instruments, Foster City, CA, USA) and imaged using a confocal microscope (Zeiss 5 Live, Oberkochen, Germany, 20x objective). Fibers were dialyzed with the rhod-2-containing internal solution. Experimental temperature was 20-22°C and the holding potential was

-80 mV. Pipette resistance varied between 1 and 2 MΩ. Correction for linear capacitive currents was performed by analog compensation. The peak current *versus* voltage relationship for I_{Ca} was fitted with:

$$I = (V_m - V_{Ca}) * G(V_m) \quad \text{(Eqn. 2)}$$

where V_m is the transmembrane potential, V_{Ca} is the estimated equilibrium potential for Ca, and $G(V_m)$ is the voltage dependence of the conductance given as:

$$G(V_m) = G_{max} / (1 + \exp(-(V_m - V_{50})/k)) \quad \text{(Eqn. 3)}$$

where G_{max} is the maximal conductance, V_{50} is the potential where the conductance is half of G_{max}, and k is the slope factor. All currents and the maximal conductance were normalized to fiber capacitance to take the size of the individual fibers into account.

External bath solution (in mM): 140 TEA-CH3SO3, 2 $CaCl_2$, 2 $MgCl_2$, 10 Hepes, 1 4-AP, 0.001 TTX (citrate), and 0.05 BTS (N-benzyl-p-toluene sulphonamide; Sigma-Aldrich). pH was adjusted to 7.2 with TEA-OH and osmolarity was adjusted to 320 mOsm with TEA methanesulfonate. Internal (pipette) solutions (mM): 110 N-methylglucamine, 110 L-glutamic acid, 10 EGTA, 10 Tris, 10 glucose, 5 Na ATP, 5 phosphocreatine Tris, 0.1 rhod-2, 3.56 $CaCl_2$, and 7.4 mM $MgCl_2$ were added for a nominal 1 mM [Mg^{2+}] and 100 nM [Ca^{2+}]. pH was set to 7.2 with NaOH and osmolarity to 320 mOsm with N-methylglucamine. Normal Tyrode's solution (in mM): 137 NaCl, 5.4 KCl, 0.5 $MgCl_2$, 1.8 $CaCl_2$, 11.8 Hepes-NaOH, 1 g/l glucose, pH 7.4).

SOCE measurement

Isolated FDB fibers loaded with the Ca^{2+} sensitive dye fluo-8 AM (4 µM, 20 min, room temperature) were imaged with a laser scanning confocal microscope (Zeiss 5 Live, Oberkochen, DE) and subjected to multiple manual solution exchanges. Changes in the fluorescence were recorded in the presence or absence of [Ca^{2+}]e following the application of a releasing cocktail and presence of a SOCE inhibitor (10 µM BTP2) and/or 1 µM nisoldipine, a potent L-type Ca^{2+} channel blocker. Following the manual delimitation of the cell border, the change of [Ca^{2+}]i was calculated as ΔF/F0, where ΔF was calculated over the cell, while F0 next to cell. "Releasing cocktail" (in mM): 0.4 4-chloro-M-cresol (4-CMC), 0.004 thapsigargin (TG), and 0.05 BTS. In some experiments, the cells were preincubated with 1 µM nisoldipine and/or 10 µM BTP2.

Elementary calcium events

Isolated intact mouse skeletal muscle fibres from the FDB were loaded with 5 µM Fluo-8 AM for 20 min at RT. This solution was then replaced by normal Tyrode's solution. Images were captured with a Zeiss LSM 510 LIVE confocal microscope (Zeiss, Oberkochen, DE) equipped with a 40x oil immersion objective (NA=1.3). Fluo-8-AM was excited with the 488-nm line of an argon laser and the emitted fluorescent light was measured at wavelengths >505 nm. 15 min following application of the recording solution, series of 200 512×512 (x,y) images captured every 67 ms were collected in each tested fibre. Test experiments were carried out in the presence of 10 µM nisoldipine in the recording solution. In some cases the recording solution contains 1.8 mM calcium.

Detection of calcium release events and their analysis were performed using methods and algorithms described previously by (Szabo et al., 2010).

Immunostaining and image processing

Muscles were isolated from 6 month old mice and embedded in Tissue Tek and freshly frozen in isopentane cooled to -80°C. Frozen muscles were stored at -80°C and transferred to -20°C one day before sectioning. Cryosections of 8 µm thickness were prepared and stored at -80°C till further use. Before immunostaining, cryosections were thawed and air dried at room temperature (RT) for 30 min. Then the muscle sections were incubated in blocking buffer consisting of 5% normal goat serum in PBS containing 1% bovine serum albumin (BSA) and 0.5% Triton X-100 (PBS/BSA/Triton) or in M.O.M blocking solution (Vector Laboratories, Burlingame, CA, USA) for 1 h at RT. Next the sections were incubated in primary antibodies (Table S2) overnight at 4°C. On the following day the sections were washed in PBS/BSA/Triton thrice at interval of 10 min and then stained with goat anti-mouse IgG-Alexa Fluor 594 or goat anti-mouse IgM-Alexa Fluor 594 (1:4000; Invitrogen) for 1 h at RT. After washing with PBS/BSA/Triton thrice at intervals of 10 min, the sections were mounted in Vectashield (Vector Laboratories, Burlingame, CA, USA). Samples were analyzed on a confocal microscope (TCS SP5, Leica microsystems, Wetzlar, DE) using a 40X objective (1.25 NA) and 16 bit images were acquired with the LasAF acquisition software (Leica microsystems, Wetzlar, DE). Figures were arranged in Adobe Photoshop CS6, and where necessary linear adjustments were performed to correct black level and contrast.

For fiber type analysis, all fibers within the entire muscle/cross-section were characterized. Fibers stained with specific antibodies against MHCs were counted in each section. For hybrid fibers serial cross-sections were analyzed simultaneously to locate the fibers stained with more than one

antibody. Fiber counts and percentages of fiber types were performed with Metamorph software (Molecular Devices, Sunnyvale, CA, USA).

SDH staining and analysis

Frozen sections of Sol and EDL were air dried for 30 min at RT and incubated in 0.2 M phosphate buffer (pH 7.4), 0.1 M succinic acid and 1.2 mM nitroblue tetrazolium for 1 h in a humidity chamber. Following incubation the slides were washed with milliQ water for 3 min and dried in methanol (Roth, Karslruhe, DE) for 2 min. The slides were then mounted in DPX mounting medium. Preparations were analyzed on an AxioImager microscope (Carl Ziess, Oberkochen, DE) using 25X (0.8 NA) and 40X (1.25 NA) objectives. 12-bit images were acquired with the SPOT Idea 1.3 Mp Color Mosaic Camera (SPOT Imaging solutions; Diagnostic Instruments Inc., Sterling Heights, MI, USA) and Spot Idea software (Version 4.6). The images were first converted to black and white tiff images in ImageJ (U.S. National Institutes of Health, Bethesda, MD, USA). Then the staining intensity of each fiber was measured using Metamorph software (Molecular Devices, Sunnyvale, CA).

Electron Microscopy and Morphometry

Sol and EDL muscles were dissected from two matched wildtype and $Ca_V1.1\Delta E29$ mouse pairs 4 and 5 months of age, immediately fixed with 3.5% glutaraldehyde in 0.12 M Na-Cacodylate buffer and processed for transmission electron microscopy as previously described in (Hess et al., 2000).

Longitudinal sections of the muscles were systematically imaged across muscle fibers and at two levels of each fiber. Thirty to forty images of each condition were analyzed using the *Metamorph* software (Molecular Devices, Sunnyvale, CA). The persons taking the images and conducting the analysis were both “blinded” with regard to the experimental condition. In each image a region was traced along the myofibril bundles and the Z-lines. Within these regions healthy mitochondria were traced to measure the size of the mitochondria and the total area covered by healthy mitochondria. From these data the fractional content of healthy mitochondria, the percentage of damaged mitochondria, and the average mitochondrial size were calculated. To exclude a possible influence of contractile state and sectioning plane on the analysis, the sarcomere length was measured and the sarcomeres in each region were counted so that the number of good and damaged mitochondria per sarcomere could be calculated. Because these controls gave the same results as when expressed as fraction of the analyzed area, they are not shown.

Protein extraction and Western blotting

Mouse Sol and EDL were isolated from 6 month old wildtype and knockout ($Ca_V1.1\Delta E29$) mice and snap frozen in liquid nitrogen. Then the frozen muscle was ground into powder using a mortar and pestle. The powder was homogenized in RIPA buffer composed of 1% Igepal, 50 mM Tris HCl, 150 mM NaCl, 0.1% SDS, 10 mM NaF and 10% glycerol to extract all the protein. The homogenized samples were centrifuged at 12,000 rpm for 15 min at 4°C. The supernatant containing the whole protein was collected. For separation of the cytoplasmic and nuclear fractions a different procedure was used as described previously (Dimauro et al., 2012). Protein concentrations were determined using the Pierce™ BCA Protein Assay Kit (Thermo Fisher Scientific Inc., Rockford, IL, USA) and measured with the NanoDrop 2000 (Thermo Fisher Scientific Inc., Rockford, IL, USA). A standard curve was determined with different concentrations of bovine serum albumin (BSA) every time protein extraction was done. 20-40 µg of protein was loaded per lane onto 6-10% Bis-Tris Gel and separated at 196 V, 40 mA for 50-60 min. The blot was performed at 25 V, 100 mA for 3 h at 4°C with a semidry-blot system (Roth, Karslruhe, DE). Primary antibodies were applied overnight at 4°C and incubation with HRP-conjugated anti-mouse or anti-rabbit secondary antibody (1:5000, Pierce) was done for 1h at RT. The primary antibodies used were as follows: Mouse antibodies against $Ca_V1.1$ (1:1000, MA3-920, Thermo Fisher Scientific), phospho-CaMKII (1:1000, #12716, Cell Signaling Technology, MA, USA), HDAC4 (1:2000, #2072, Cell Signaling Technology, MA, USA), NFATc1 (1:500, sc-13033, Santa Cruz Biotechnology, Heidelberg, DE), Histone H3 (1:2000, Cell Signaling Technology, MA, USA), GAPDH (1:100,000, SC32233, Santa Cruz Biotechnology, Heidelberg, DE) and α-tubulin (1:1000, ab7291, Abcam, Cambridge, UK). The development was performed with SuperSignal® West Pico Chemiluminiscent Substrate (Thermo Fisher Scientific Inc., Rockford, IL, USA) and ImageQuant Las 4000 (GE Healthcare Europe GmbH, Vienna, AT) was used to visualize the bands. Quantification of the bands was done with ImageJ (U.S. National Institutes of Health, Bethesda, MD, USA, imagej.nih.gov/ij) software (mean ± SEM, N=3, $p > 0.05$, * $p < 0.05$, *** $p < 0.001$).

Calcineurin activity assay

Mouse Sol and EDL tissue samples were frozen in liquid N_2 at the time of dissection, stored at -80°C and homogenized in a buffer containing 0.1 M sucrose, 46 mM KCl, 0.5 % BSA, 100 mM Tris-HCl (pH 7.4) and EDTA-free protease inhibitors (SIGMA). Protein determination were carried out as described before (Lontay et al., 2004). Calcineurin (protein phosphatase 2B; PP2B) activity was determined by the Calcineurin Phosphatase Activity Colorimetric Assay (Abcam) following the the manufacturer's instructions. Shortly, PP2B activity of the skeletal muscle lysates was measure by using RII

phosphopeptide substrate. The quantity of the free-phosphate liberated was detected by Malachite green assay at 620 nm and it was correlated with the PP2B activity. Human recombinant calcineurin was applied as a positive control. To discriminate between the contribution of other protein phosphatases lysates were incubated with 100 nM okadaic acid (OA; a specific protein phosphatase 1 and 2A inhibitor) with or without EGTA before the enzyme activity measurement. Calcineurin activity was calculated as the difference of the enzyme activities measured in the OA-treated and the OA/EGTA-treated lysates and was normalized in each case to the total protein concentration.

Statistical analysis.

A two way ANOVA with Bonferroni post hoc test was used for homecage activity and fiber type analysis (Fig. 1A and 1B). A one way ANOVA was used for the other behavioral tests. The Student's t-test was used to calculate the statistical significance for fiber type analysis in SDH staining, mitochondria analysis in electron microscopy and all tests for contractile properties. Levels of significance for t-test and ANOVA are indicated as * $p < 0.05$; ** $p < 0.01$; *** $p < 0.001$. The statistical analysis was performed with GraphPad Prism (GraphPad Software, La Jolla, CA, USA).

Supplemental References:

Benjamini, Y. and Hochberg, Y. (1995). Controlling the false discovery rate: a practical and powerful approach to multiple testing. *J Roy Statist Soc Ser B* **57**, 289-300.

Bindreither, D., Ecker, S., Gschirr, B., Kofler, A., Kofler, R. and Rainer, J. (2014). The synthetic glucocorticoids prednisolone and dexamethasone regulate the same genes in acute lymphoblastic leukemia cells. *BMC genomics* **15**, 662.

Bodnar, D., Geyer, N., Ruzsnavszky, O., Olah, T., Hegyi, B., Sztretye, M., Fodor, J., Dienes, B., Balogh, A., Papp, Z., Szabo, L., Muller, G., Csernoch, L. and Szentesi, P. (2014)Hypermuscular mice with mutation in the myostatin gene display altered calcium signaling. *Journal of Physiology* **592**, 1353-1365.

Csernoch, L., Pouvreau, S., Ronjat, M. and Jacquemond, V. (2008). Voltage-activated elementary calcium release events in isolated mouse skeletal muscle fibers. *The Journal of membrane biology* **226**, 43-55.

Dimauro, I., Pearson, T., Caporossi, D. and Jackson, M. J. (2012). A simple protocol for the subcellular fractionation of skeletal muscle cells and tissue. *BMC research notes* **5**, 513.

Gentleman, R. C., Carey, V. J., Bates, D. M., Bolstad, B., Dettling, M., Dudoit, S., Ellis, B., Gautier, L., Ge, Y., Gentry, J., et al. (2004). Bioconductor: open software development for computational biology and bioinformatics. *Genome biology* **5**, R80.

Hess, M. W., Schwendinger, M. G., Eskelinen, E. L., Pfaller, K., Pavelka, M., Dierich, M. P. and Prodinger, W. M. (2000). Tracing uptake of C3dg-conjugated antigen into B cells via complement receptor type 2 (CR2, CD21). *Blood* **95**, 2617-2623.

Lontay, B., Serfozo, Z., Gergely, P., Ito, M., Hartshorne, D. J. and Erdodi, F. (2004). Localization of myosin phosphatase target subunit 1 in rat brain and in primary cultures of neuronal cells. *The Journal of comparative neurology* **478**, 72-87.

Oddoux, S., Brocard, J., Schweitzer, A., Szentesi, P., Giannesini, B., Brocard, J., Faure, J., Pernet-Gallay, K., Bendahan, D., Lunardi, J., et al. (2009). Triadin deletion induces impaired skeletal muscle function. *The Journal of biological chemistry* **284**, 34918-34929.

Rainer, J., Lelong, J., Bindreither, D., Mantinger, C., Ploner, C., Geley, S. and Kofler, R. (2012). Research resource: transcriptional response to glucocorticoids in childhood acute lymphoblastic leukemia. *Molecular endocrinology* **26**, 178-193.

Schlick, B., Flucher, B. E. and Obermair, G. J. (2010). Voltage-activated calcium channel expression profiles in mouse brain and cultured hippocampal neurons. *Neuroscience* **167**, 786-798.

Smyth, G. K. (2004). Linear models and empirical bayes methods for assessing differential expression in microarray experiments. *Statistical applications in genetics and molecular biology* **3**, Article3.

Szabo, L. Z., Vincze, J., Csernoch, L. and Szentesi, P. (2010). Improved spark and ember detection using stationary wavelet transforms. *Journal of theoretical biology* **264**, 1279-1292.

Sztretye, M., Yi, J., Figueroa, L., Zhou, J., Royer, L. and Rios, E. (2011). D4cpv-calsequestrin: a sensitive ratiometric biosensor accurately targeted to the calcium store of skeletal muscle. *The Journal of general physiology* **138**, 211-229.

Truett, G. E., Heeger, P., Mynatt, R. L., Truett, A. A., Walker, J. A. and Warman, M. L. (2000). Preparation of PCR-quality mouse genomic DNA with hot sodium hydroxide and tris (HotSHOT). *BioTechniques* **29**, 52, 54.

Supplementary Tables:

Table S1: Oligonucleotides for real time PCR

Gene	Ref. no.	Method	Forward primer (5'-3')	Reverse primer (5'-3')	Probe
CACNA1S	NM_001081023	TaqMan	gttacatgagctggatcacacag	atgagcatttcgatggtgaag	
CACNA1S-E29	NA	TaqMan	ctaatcgtcatcggcagcat	tctcatctgggtcatcgatct	attgacgtcatcctgagc
CACNA1S+E29	NA	TaqMan	ctaatcgtcatcggcagcat	ctccacccaggcaatacagt	attgacgtcatcctgagc
Ppargc1a	NM_008904	TaqMan	ctccatctgtcagtgcatca	ccaaccagtacaacaatgagc	agggcaatccgtcttcatccacg
Six 1	NM_009189	TaqMan	gagagagttgattctgcttgttg	ggtcagcaactggttaagaac	cgaggccaaggaaagggagaaca

Table S2: Antibodies for immunostaining

Fibre type	Primary Antibody*	Concentration	Secondary Antibody	Concentration
I	BA-D5	1:2000	Anti-mouse IgG Alexa 594	1:4000
IIA	SC-71	1:2000	Anti-mouse IgG Alexa 594	1:4000
IIB	BF-F3	1:2000	Anti-mouse IgG Alexa 594	1:4000
IIX	6H1	1:200	Anti-mouse IgM Alexa 594	1:4000

*All primary antibodies were purchased from Developmental Studies Hybridoma Bank, Iowa, USA.

Supplementary Figures:

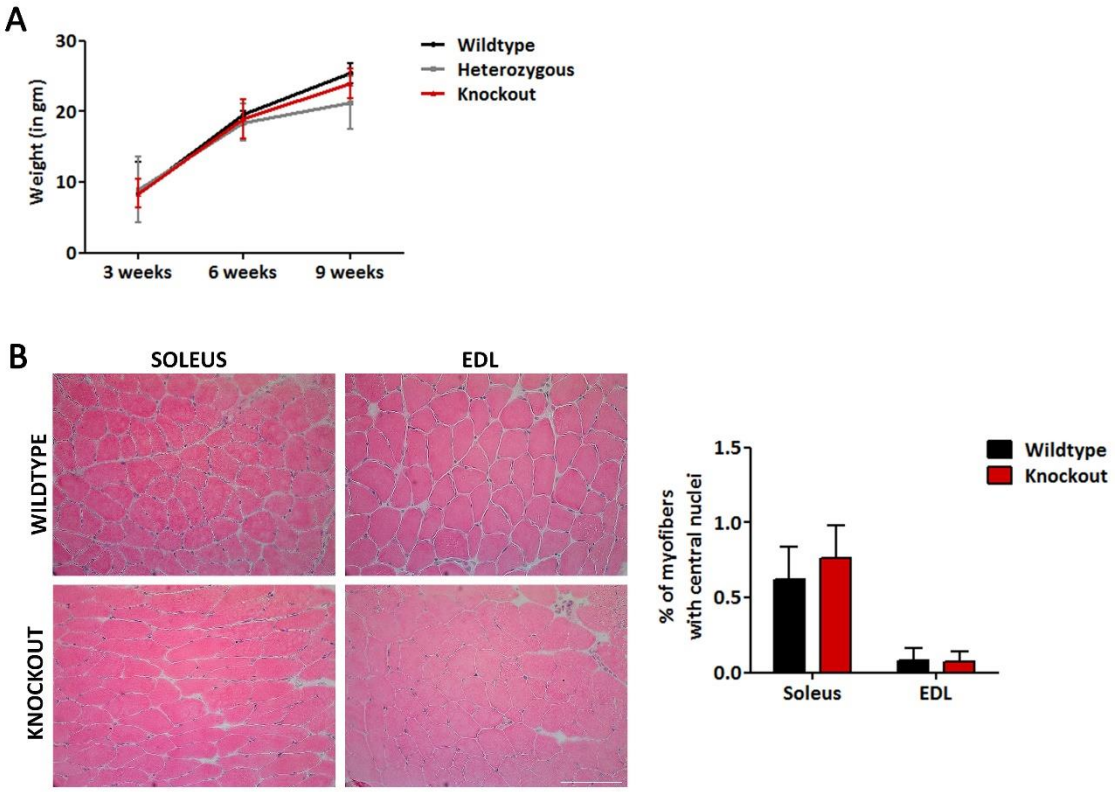

Figure S1. Phenotype of $Ca_V1.1\Delta E29$ mice: Normal weight gain and muscle histology. (**A**) The increase of body weight measured at 3, 6 and 9 weeks of age was similar in $Ca_V1.1\Delta E29$ mice compared to the wildtype and heterozygous siblings (mean ± SEM, N=15-37, $p>0.05$). (**B**) Haematoxylin and eosin stained cryosections of soleus and EDL muscles at 6 months revealed no centrally located nuclei in $Ca_V1.1\Delta E29$ muscle fibers (Scale bar: 100µm). Quantitative analysis showed no significant differences between $Ca_V1.1\Delta E29$ and wildtype mice (mean ± SEM, N=3, $p > 0.05$).

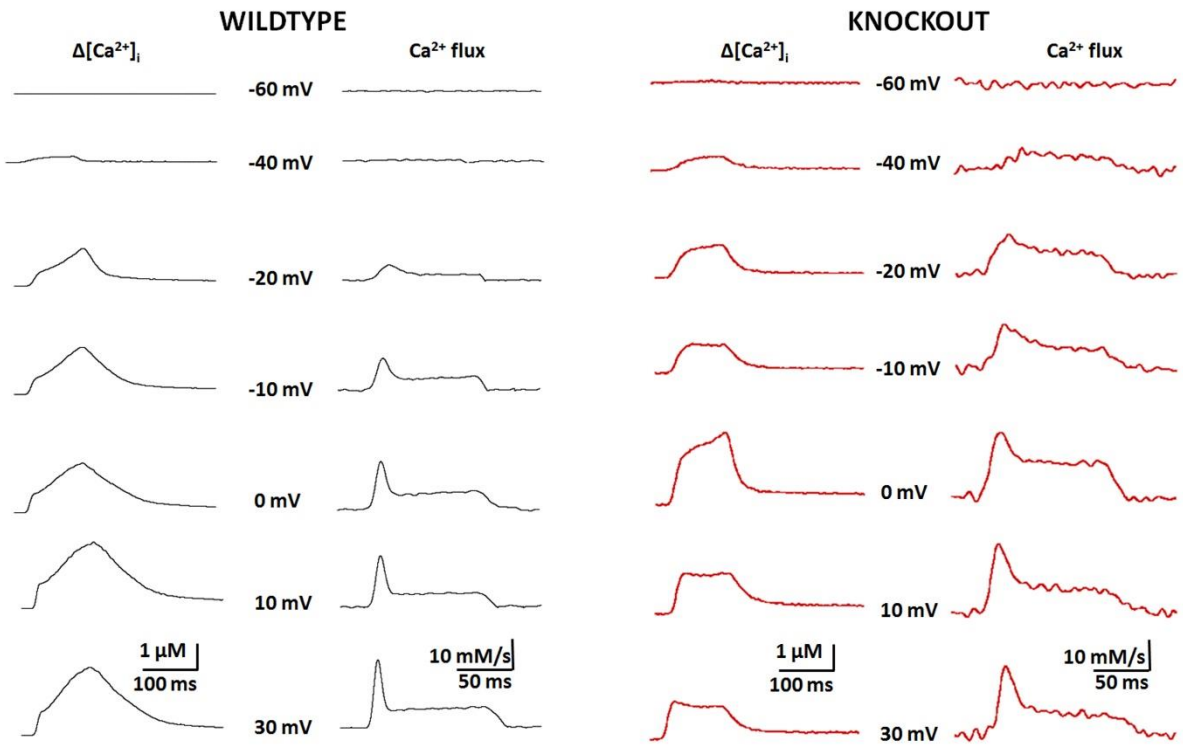

Figure S2. Voltage-dependence of calcium transients and calcium fluxes in FDB muscle fibers of wildtype and $Ca_V1.1\Delta E29$ mice. Calcium transients were recorded in voltage-clamped, Rhod-2 loaded FDB fibers and calcium fluxes were calculated as described in the extended materials and methods. At intermediate voltages the plateau flux relative to the peak is substantially higher in $Ca_V1.1\Delta E29$ than in wildtype controls, indicating a strong contribution of voltage-dependent calcium influx to the myoplasmic calcium transients.

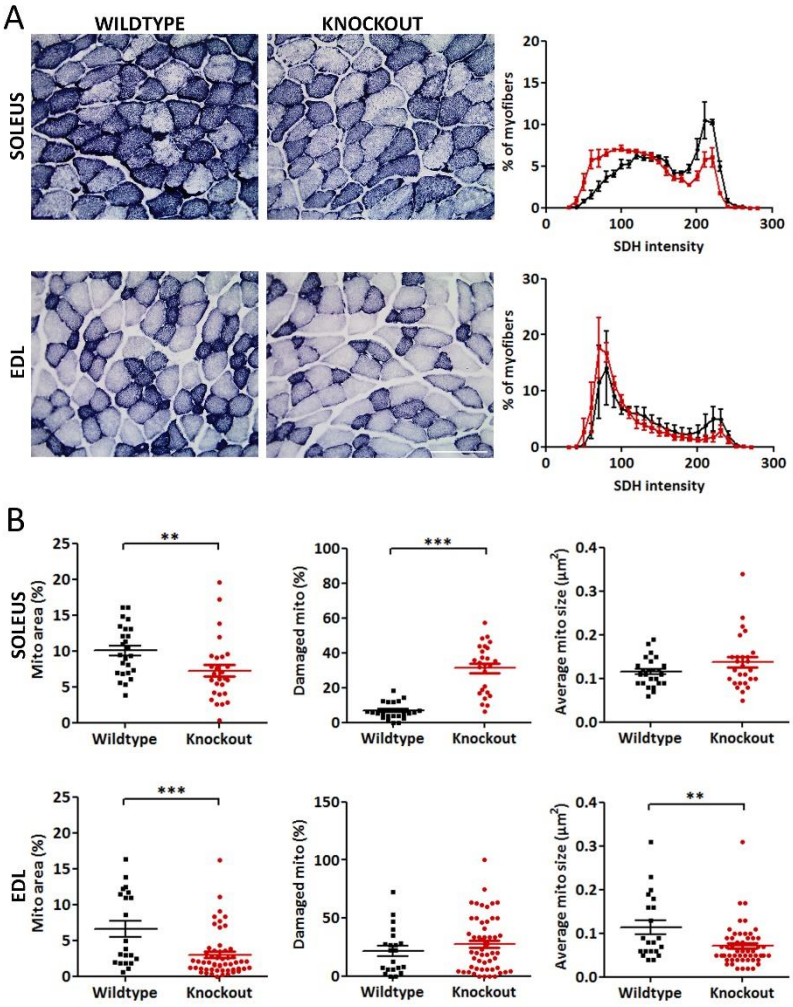

Figure S3. SDH staining and electron microscopy analysis demonstrates reduced mitochondrial function and content in $Ca_V1.1\Delta E29$ muscles. (**A**) SDH activity was analyzed in sections of 12 months old wildtype (black) and $Ca_V1.1\Delta E29$ (red) mice (Scale bar: 100 µm). Staining intensity was measured in each fiber profile and plotted in intensity distribution diagrams. SDH activity is significantly reduced in $Ca_V1.1\Delta E29$ soleus and EDL muscles visible as left shift in the distribution curves (mean ± SEM, N=3 (**B**) (Biological replicate of experiment shown in Fig. 6C and D, and corresponding to the second data set given in Results). Morphometric analysis demonstrates significantly decreased fraction of the area occupied by intact mitochondria in both soleus ($p<0.01$) and EDL ($p<0.001$) muscles of $Ca_V1.1\Delta E29$. Mitochondrial size is decreased in $Ca_V1.1\Delta E29$ EDL ($p<0.01$) and the fraction of damaged mitochondria increased ($p<0.001$) in $Ca_V1.1\Delta E29$ soleus muscles (mean ± SEM, N=2).

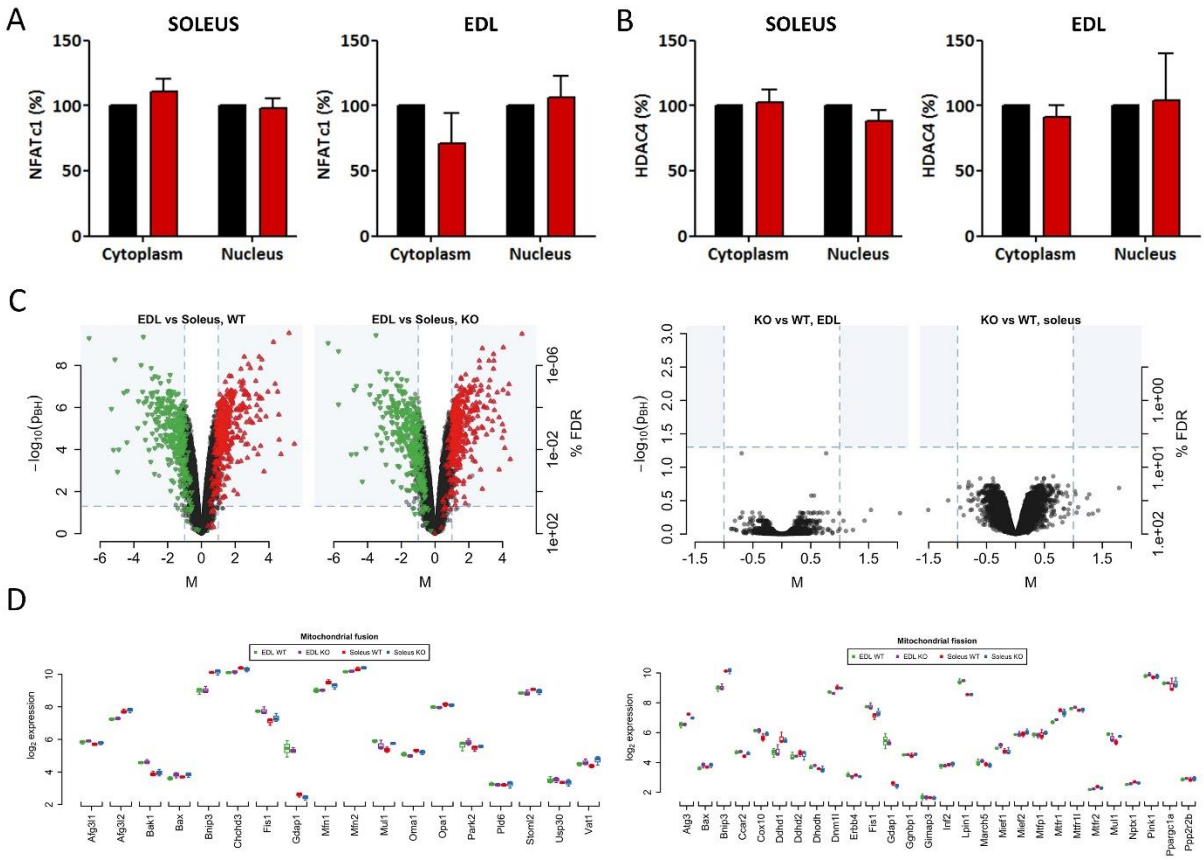

Figure S4. Expression of the transcriptional regulators NFATc1 and HDAC4 and the gene expression profile were not altered in $Ca_V1.1\Delta E29$ mice. (**A, B**) Quantitative analysis of NFATc1 and HDAC4 Western blots shown in Fig. 7 revealed no significant differences in cytoplasmic or nuclear fractions of soleus and EDL muscles of 5-6 month old $Ca_V1.1\Delta E29$ mice and wildtype controls (mean ± SEM, $p > 0.05$, N=3). (**C**) Volcano plots of *Affymetrix* gene chip analysis show differentially expressed genes in soleus and EDL muscles, but differential expression in 6 month old wildtype and $Ca_V1.1\Delta E29$ muscles did not reach significance. Both soleus and EDL muscles were pooled from three female $Ca_V1.1\Delta E29$ and wildtype mice six months of age (mean ± SEM, $p>0.05$, N=3). (**D**) Expression of genes linked to mitochondrial fusion (left) and fission (right) was not altered in $Ca_V1.1\Delta E29$ muscles.